(12) INTERNATIONAL APPLICATION PUBLISHED UNDER THE PATENT COOPERATION TREATY (PCT)

(19) World Intellectual Property Organization
International Bureau

(43) International Publication Date
26 May 2005 (26.05.2005)

PCT

(10) International Publication Number
WO 2005/047575 A1

(51) International Patent Classification[7]: C30B 30/02, B01J 13/00

(21) International Application Number: PCT/SG2004/000369

(22) International Filing Date: 12 November 2004 (12.11.2004)

(25) Filing Language: English

(26) Publication Language: English

(30) Priority Data:
60/519,573 12 November 2003 (12.11.2003) US

(71) Applicant *(for all designated States except US)*: **NATIONAL UNIVERSITY OF SINGAPORE** [SG/SG]; 10 Kent Ridge Crescent, Singapore 119260 (SG).

(72) Inventors; and

(75) Inventors/Applicants *(for US only)*: **ZHANG, Keqin** [CN/SG]; Dover Road, BLK 02, #02-326, Singapore 130002 (SG). **LIU, Xiang, Yang** [NL/SG]; 111 Clementi Road, Block C, #05-07, Singapore 129792 (SG).

(74) Agent: **DREW & NAPIER LLC**; Intellectual Property Department, 20 Raffles Place #17-00, Ocean Towers, Singapore 048620 (SG).

(81) Designated States *(unless otherwise indicated, for every kind of national protection available)*: AE, AG, AL, AM, AT, AU, AZ, BA, BB, BG, BR, BW, BY, BZ, CA, CH, CN, CO, CR, CU, CZ, DE, DK, DM, DZ, EC, EE, EG, ES, FI, GB, GD, GE, GH, GM, HR, HU, ID, IL, IN, IS, JP, KE, KG, KP, KR, KZ, LC, LK, LR, LS, LT, LU, LV, MA, MD, MG, MK, MN, MW, MX, MZ, NA, NI, NO, NZ, OM, PG, PH, PL, PT, RO, RU, SC, SD, SE, SG, SK, SL, SY, TJ, TM, TN, TR, TT, TZ, UA, UG, US, UZ, VC, VN, YU, ZA, ZM, ZW.

(84) Designated States *(unless otherwise indicated, for every kind of regional protection available)*: ARIPO (BW, GH, GM, KE, LS, MW, MZ, NA, SD, SL, SZ, TZ, UG, ZM, ZW), Eurasian (AM, AZ, BY, KG, KZ, MD, RU, TJ, TM), European (AT, BE, BG, CH, CY, CZ, DE, DK, EE, ES, FI, FR, GB, GR, HU, IE, IS, IT, LU, MC, NL, PL, PT, RO, SE,

[Continued on next page]

(54) Title: COLLOIDAL STRUCTURE AND METHOD OF FORMING

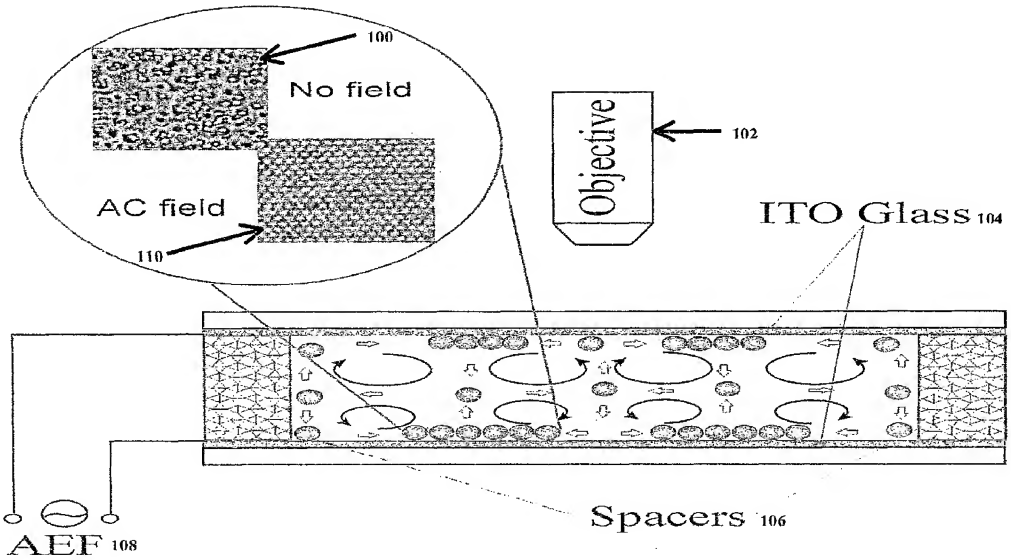

(57) Abstract: Here we demonstrate a method of assembling charged colloidal particle driven by an alternating electric field. This system allows us to have direct imaging and in-situ observation of nucleation, and in particular the pre-nucleation process, which are explored in real space by a light microscope. By following their evolution, a set of important pararneters of nucleation can be measured under different driving forces. The advantages of our system are direct visualization of the nucleation process for colloidal particle assembly and better control of the level of perfection of the crystals based on a well-defined driving force.

WO 2005/047575 A1

SI, SK, TR), OAPI (BF, BJ, CF, CG, CI, CM, GA, GN, GQ, GW, ML, MR, NE, SN, TD, TG).

Published:

— *with international search report*

For two-letter codes and other abbreviations, refer to the "Guidance Notes on Codes and Abbreviations" appearing at the beginning of each regular issue of the PCT Gazette.

"COLLOIDAL STRUCTURE AND METHOD OF FORMING"

BACKGROUND OF THE INVENTION

1. Field of the Invention

The present invention relates to 2D and 3D colloidal structures particularly though not solely to a method of forming colloidal crystals of large size, high stability and low defects.

2. Description of the Prior Art

Large and high quality colloidal crystals find application in for example the templating of photonic crystal, optical switching, drug delivery and biosensors.

The reversible aggregation of ordered 2D/3D colloidal particles into planar particles adjacent to an electrode surface may be induced by an electric field that is applied normal to the electrode surface. It has been demonstrated that the underlying attractive interaction between particles is mediated by electrokinetic flow (Yeh, Seul and Shraiman, "Assembly of ordered colloidal aggregates by electric field induced fluid flow", Nature 386,57-59, (1997) and US patent no. 6468811).

Trau, et al (US patent 6033547 and references herein) describe the apparatus and method for assembling the particles into crystalline structures induced by a DC field and also mentioned the effects of an AC field. Gong Tieying, David T. Wu and David W. M. Marr (Langmuir 2003, 19, 5967-5970, "Electric field-reversible three-dimensional colloidal crystals" and Langmuir 2002, 18, 10064-10067, "Two-dimensional electrohydrodynamically induced colloidal phases") used an AC electric field to produce 2D and 3D colloidal assembly.

In all above works, the prior art suffers from discontinuous colloidal crystals, with small domains and many defects. Thus far a large (millimetre) and high quality colloidal crystal has never been achieved. Also no quantitative control of the two-dimensional (2D) or three-dimensional (3D) colloidal crystallization has been performed from the view of nucleation and growth.

SUMMARY OF THE INVENTION

It is therefore an object of the present invention to provide a colloidal structure or method or process of forming colloidal structures which goes some way to overcoming the above mentioned disadvantages in the prior art.

Accordingly in a first aspect the present invention may be broadly said to consist in a

method of identifying optimum electric field conditions for forming a colloidal structure of particles within a solution comprising the steps of:

applying an AC electric field to the solution and varying the frequency,

applying an AC electric field to the solution and varying the magnitude,

identifying an optimum range of frequencies and magnitudes to form said colloidal particle structure.

Wherein said optimum range is at least partially bounded by at least one phase transition.

Wherein said optimum range of magnitude is bounded by an infinite order phase transition.

Wherein said optimum range of frequency is bounded by one or more second order phase transitions.

Wherein said optimum range is characterised by a particle spacing less than a predetermined threshold.

Wherein said optimum range is characterised by more than two particles spaced less than a predetermined threshold from one another.

Wherein said optimum range is further characterised by a particle to particle bond angle within a predetermined range.

Wherein said optimum range is characterised by said particles not being fluid or disordered.

Wherein said optimum range is characterised by said particles not being unstable or where the electric field is so high that chemical reaction occur.

Wherein said optimum range is further characterised by identifying the boundaries between ideally formed and non ideally formed structures.

Wherein said optimum range is further characterised by identifying the type or order of said phase transitions.

Wherein said type or order are characterised by determining the pair correlation function $g(r)$ and the bond-orientational correlation function $g_6(r)$ from the respective equations:

$$g(r) = \langle \rho_G(0)\rho_G(r)\rangle, \quad \rho_G(r) = \sum_{i=1}^{N} e^{iG\cdot r_i}\delta(r - r_i)$$

$$g_6(r) = \frac{\langle \psi_6^*(0)\psi_6(r)\rangle}{\langle \delta(r_i)\delta(r_j - r)\rangle}, \quad \psi_6(r_i) = \langle \frac{1}{N}\sum_j e^{6i\theta(r_{ij})}\rangle$$

wherein G denotes a reciprocal-lattice vector of a solid, and $\theta(r_{ij})$ is the angle between the bond connecting particles i and j and an arbitrary fixed reference axis.

Wherein said type or order are determined by approximating a ln plot of the order parameters order parameters of the translational correlation length ξ_T and the power-law exponent η_6 with the function $e^{-\alpha(\sigma_E-\sigma_E^c)^\beta}$, wherein α, β are the fitting parameters.

Wherein said optimum range is further comprised of a oscillating chain-like phase.

Wherein said optimum range is further comprised of a vortex ring phase.

Wherein said optimum range is further comprised of a 3D aggregation phase.

Wherein said optimum range is further comprised of a 2D hexagonal close packed phase.

In a second aspect the present invention may be broadly said to consist in a method or process of preparing a substantially crystalline colloidal structure (colloidal crystal) between electrodes comprising or including the steps of:

selecting a colloid system from which the colloidal crystal will be formed,

selecting a electrode AC voltage magnitude and frequency from a preferred domain of magnitude against frequency which gives rise to a substantially stable colloidal crystal,

providing an electric field from said electrodes using said selection to prepare the colloidal crystal, which may be in substantially two dimensions or substantially in three dimensions, on or proximal to the surface of one electrode.

Wherein said preferred domain of electrode potential against frequency is compiled by conducting at least three experiments/runs of measuring electrode potential against frequency herein there are at least two different potentials applied/used/measured and there are at least two different frequencies applied/used/measured.

Wherein said preferred domain of electrode potential against frequency is compiled according to any one of the preceding clauses.

Wherein the step of generally identifying the domain of electrode potential against frequency includes using the results of the at least three experiments/runs to prepare (whether very generally or in detail) a phase diagram showing (whether very generally or very accurately) regions of ordered and disordered colloidal behavior.

Wherein the step of preparing the phase diagram involves observing the pattern of the colloidal assembly with each experiment /run.

Wherein the at least three experiments/runs are obtained by the acts of (in no particular order)

holding the AC voltage magnitude substantially constant, varying the frequency and observing the pattern of the colloidal assembly at least once,

holding the AC voltage frequency substantially constant, varying the voltage and

observing the pattern of the colloidal assembly at least once.

Wherein the step of generally identifying said domain of electrode potential against frequency includes using the results of the at least three experiments/runs to prepare (whether very generally or in detail) a phase diagram showing (whether very generally or very accurately) one or more of:

a domain of oscillating chain like behavior of the colloid system

a domain of vortex ring behavior of the colloid system

a domain of three dimensional aggregation, between the electrodes, within the colloid system

a domain of disordered behavior of the colloid system

a domain of hexagonally close packed two dimensional formation of a colloidal crystal, between the electrodes, within the colloid system

a domain of instability or of the solution chemically reacting.

Wherein the colloidal crystal may be substantially planar (in two dimensions).

Wherein the colloidal crystal may be in three dimensions.

Wherein the colloidal crystal may be a mixture of two and three dimension.

Wherein the step of selecting the colloid system includes selecting the solvent, concentration, pH, and diameter of colloidal spheres.

Wherein the step of preparing the phase diagram involves one or more of:

knowledge of the distance of separation between the electrodes,

knowledge of the volume fraction of the colloids,

knowledge of the zeta potential of the colloids,

knowledge of the size of the colloids.

Wherein the diameter of colloidal crystals is at least 100μm.

In a third aspect the present invention may be broadly said to consist in a colloidal crystal prepared substantially according to the method or process as claimed in any one of the preceding clauses.

To those skilled in the art to which the invention relates, many changes in construction and widely differing embodiments and applications of the invention will suggest themselves without departing from the scope of the invention as defined in the appended claims. The disclosures and the descriptions herein are purely illustrative and are not intended to be in any sense limiting.

The invention consists in the foregoing and also envisages construction which the

following gives examples.

BRIEF DESCRIPTION OF THE DRAWINGS

One preferred form of the present invention will now be described with reference to the accompanying drawings in which

Figure 1a is a block diagram of the experimental setup for assembling two-dimensional colloidal particles by controlling the alternating electric field.

Figure 1b is a graph of the structure of the 2D colloidal crystal is quantified by the pair correlation function g(r). The position of the first peak of g(r) corresponds to a fixed centre to centre distance between neighbouring particles. The effect on the colloidal crystal structure caused by varying the field strength from 0.9Vp-p to 2.8Vp-p, while keeping the frequency fixed at 600Hz, is illustrated by plotting the g(r) against r/a at 2.8Vp-p, 1.5Vp-p, 0.9Vp-p. The variation of the position of the first peak of the g(r), which is independent of the shape of the peak with respect to Vp-p, is shown in the inset by the slope of the plot of the first peak position against the voltage.

Figure 1c is a graph of the absence of any effect on the colloidal crystal structure despite the variation of the frequency from 450Hz to 2500Hz, while keeping the field strength fixed at 2.4Vp-p, is illustrated by plotting the g(r) against r/a at 0.4kHz, 1kHz, 1.5kHz. The constancy of the position of the first peak of g(r) with respect to the frequency, is shown in the inset by the horizontal least-square linear fit of the plot of the first peak position against frequency.

Figure 1d is a graph of the supersaturation is examined by the fraction of the area of the electrode occupied by colloidal particles versus the frequency while keeping the voltage fixed at 2.4Vp-p.

Figure 2 is snapshots of the pre-nucleation process at time multiples of t_o =0.293s, where t_o is the timing interval of the images. The nuclei indicated by the yellow circles will be disappearing or shrinking; the nuclei indicated by the red circles will grow and gradually increase in size. The radius of red and yellow circles equals to the critical radius r_c at the given supersaturation (2.4Vp-p, 600Hz). (a), $t=14t_o$. (b), $t=34t_o$. (c), $t=54t_o$. (d), $t=74t_o$.

Figure 3a is a graph of the typical size distribution of subcritical nuclei at different times (2.4Vp-p, 600Hz). The inset corresponds to t=20.8s.

Figure 3b is a graph of n*(t) versus time. After reaching the induction time τ, n*(t) becomes stable, thus allowing the determination of the critical size.

Figure 3c is a graph of the number of nuclei having size larger than the critical size at

different times. The nucleation rate per unit area can be obtained from the slope of a linear fit to the data points.

Figure 3d is a graph of the nucleation rate density versus supersaturation (driving force). In the main text we show how the edge energy density (line tension) can be calculated from the linear fit to the data points.

Figure 4a is view from a microscope of the solution with DC electric field at 3.2V. The FFT in the inset on the upper right corner shows the ring of diffraction.

Figure 4b is view from a microscope of the solution with AC electric field at 2.4Vp-p, 600Hz. The FFT in the inset on the upper right corner shows the uninterrupted hexagonal symmetry of the crystal.

Figure 5 is a view from a microscope of colloidal particles at the isoelectric point.

Figure 6 is a phase diagram of AC electric field strength against frequency.

Figure 7a is a plot of the translational correlational function as a function of strength σ_E.

Figure 7b is a plot of the bond-orientational correlation function as a function of strength σ_E.

Figures 8a and 8b are ln plots of the order parameters ξ_T and η_6 against the critical field strength.

Figure 9 are ln plots of the order parameters ξ_T and η_6 against the critical field strength.

Figure 10 is a phase diagram of the order-disorder phase transitions in the space of strength and frequency of an alternating electric field.

Figure 11a is a plot of bond-orientational order against field strength at a fixed frequency of 800Hz.

Figure 11b is a plot of correlation length against field strength at a fixed frequency of 800Hz.

Figure 11c is a plot of bond-orientational order against frequency at a fixed field strength of 2.8×10^4 *V/m*.

Figure 11d is a plot of correlation length against frequency at a fixed field strength of 2.8×10^4 *V/m*.

Figure 12a is a log plot of the correlation length against the critical field strength at a fixed frequency of 800Hz

Figure 12b is a plot of $\ln(\xi_T/a)$ against $\ln(f-f_c)$ in the frequency-dependant phase transition at a fixed field strength of 2.8×10^4 *V/m*.

Figure 13 is a plot of the lattice spacing of the colloidal assembly against varying frequencies and varying field strengths.

Figure 14a is a view from a microscope of 2D colloidal crystals having a diameter of 5 μm.

Figure 14b is a view from a microscope of 2D colloidal crystals having a diameter of 200 nm.

Figure 15 a graph of the Zeta Potential against pH.

DETAILED DESCRIPTION

The study of the nucleation of crystalline materials is one of the most important areas of materials sciences and technology. Although a great deal is known about the behaviour of bulk crystals, considerably less is known about their earliest stage, when they nucleate and grow from a liquid. This is mainly due to the lack of effective means for the direct measurement and the in-situ observation of the nucleation process and the nucleation kinetics. Charge-stabilized colloidal suspensions of monodispersed microspheres have been taken as a suitable model system for the study of structural phase transitions and crystal nucleation, as they show an analogous phase diagram to non-colloidal crystal growth, and the growth units are microscopically visible. Recent advances in a quantitative 3D real-space analysis of the structure and dynamics of colloids have been achieved by the confocal microscopy.

An important driver in the process identified by the applicant is the role of the thermodynamic driving force, μ/k_BT. Here μ is the difference of chemical potential between growth unit in the crystal and the liquid phases, k_B denotes Boltzmann's constant, and T is the absolute temperature. In the process of crystal growth this chemical potential difference is well defined, and hence it can be utilized to define the driving force in theoretical formations of crystal growth. However in the context of nucleation the chemical potential difference is an ill-defined quantity leading to the lack of a clear equivalent for the driving force in the nucleation process. If we were to use the aforementioned definition of driving force in the nucleation process, that would only give rise to a very rough estimate of the surface free energy and the critical size of a nucleus (up to 300% of error). In other words, the in-situ observation of the pre- and post-nucleating processes and the real time measurement of nucleation kinetics, in particular under a well-defined thermodynamic driving force, have not been achieved.

In one example the present invention will present an in-situ real space microscopic

imaging of the 2D nucleation process and the real time measurement of the kinetics for a colloidal system. In particular, the nucleation process will be observed under a well-defined supersaturation controlled by an AC electric field. The growth of dislocation-free (or perfect) crystals is controlled by the 2D nucleation mechanism. The growth of a new layer or the occurrence of steps on a perfect crystal surface will start via 2D nucleation. We will measure the cluster distribution of colloidal spheres at the pre- and post nucleation stages. The transition from the non-steady to the steady state of nucleation can be observed for the first time. Subsequently we will determine quantitatively the critical size of nuclei, the nucleation rate, the nucleation barrier of the steady state of nucleation at different supersaturations, and the line tension of a 2D colloidal crystal. As mentioned above, the high quality colloidal crystals have broad applications in different areas. Understanding of the nucleation and growth of colloidal spheres allows us to fabricate large and high quality colloidal crystals.

Example experiment strategy

In one example the present invention employs an alternating current to produce high quality two-dimensional structures. High quality in this case means that the surface exhibits molecular arrangements of a high degree of regularity, and that the domains enclosing such regular arrangements are as large as possible with a minimum amount of defects or other irregularities.

In the prior art, end-products with large lattice spacing, that is, large distances between the particles, are of relatively good quality. However, when the lattice spacing is small, the quality of the end-products of the prior art is poor. In contrast, the high quality of the end-product of the present invention is not restricted to a large lattice spacing. The invention provides not only for an improved end-product quality over a much broader range of lattice spacing than the prior art, it also provides for an optimal control of the obtained quality.

The present invention involves obtaining the ideal electric field in which the structure forms. In an example experimental strategy both the frequency and the magnitude of the applied voltage or electric field are varied, enabling the user of the invention to obtain an optimal quality under the given experimental conditions. The prior art does not apply such variation.

Also the prior art utilizes low values of voltage magnitude and voltage frequency. Thus the invention provides for a method in which higher voltages and higher frequencies can be applied than is done in the prior art. High voltages are desirable because they allow the

production of structures with short lattice spacing. In most systems tested in our experiments, the optimal quality of the end-product was obtained between 300Hz and 3 kHz, a value lying well above the maximum frequency applied in the prior art. We expect this to be true for the monodispersed system, but for the binary we expect an ordered phase in the frequency range 20k-200kHz.

The prior art also fails at low concentrations, and hence it is limited to introducing high concentrations of particles are in the solution (usually water). In contrast, the method of the present invention succeeds in producing the desired product at low concentrations. Moreover, at high concentrations the present method leads to end-products of a quality that is higher than the quality obtained by the prior art at similar concentrations.

The prior art teaches application of a single non ideal wave form as the electric field. In contrast, in the present invention the voltage wave form may be varied to provide a means of quality control. By manipulating the wave form, e.g. from sinusoidal to square-stepped or triangular-stepped, the quality of the end-product can be improved further.

The parameters which affect the formation of 2D and 3D crystals in a given application are:

- The size of colloidal spheres
- The density of colloidal spheres
- The zeta potentials of colloidal spheres
- The volume fraction of colloidal spheres in the solutions
- The type of solvent
- The pH of the solutions
- The type and the concentration of electrolytes.

Therefore changing any of these will result in different ideal conditions. One strategy is to vary the field strength E and frequency f of the applied electric field, and observe the results using optical microscopy. Using this technique it is possible to identify the range of conditions if is possible for ordered and disordered colloidal assembly.

In one embodiment the applicant has identified that the ideal conditions for a given application may be obtained by applying a customised electric field. This involves identifying at least an optimal voltage magnitude and frequency for a given type of resulting structure. Also throughout the formation these in turn may be varied and/or different wave form shapes applied depending on the desired result.

Referring to Figure 1a an example setup is shown for observing the structures resulting

from a given electric field. The variable power supply 108 may be manually or automatically varied according to AC voltage magnitude, frequency and / or waveform type. In a further example the supply may be computer of microprocessor controlled to vary the voltage according to a stored program.

Supply 108 is connected to parallel plate electrodes 104. In one example the electrodes are ITO glass which allows observation of the solution form the exterior. The electrodes are spaded by spacers 106 to give a uniform electrode gap of desired dimension.

The microscope or other optical recorder 102 is situation perpendicular to the electrode to observe formation on the electrode surfaces. For example with ideal AC field one might expect to view hexagonally close packed crystals, and without a disordered pattern 100.

A domain may be identified which defines the boundaries of electric field conditions which will allow optimum structure formation 606 as seen in Figure 6. In order to obtain the high quality order colloidal crystals, the chosen electric field 600 should not be to close to the domain boundary 602, or the density of defects will be too high. On the other hand, the field should not be too far from the phase boundary, otherwise the nucleation rate of colloidal crystals will be too high, which will lead to a multi-domain assembly (polycrystalline). Other domains could result in different structures forming. In general the liquid state 604 is undesirable. Also by applying too high a voltage an unstable state 608 occurs where the electrodes chemically react with the solution. As well this state is transient or meta-stable and is not desirable for continued use of the cell.

Within the desirable state various types of structures may be accommodated by selecting an appropriate magnitude and frequency combination. For example an ordered 3D crystal region 610 can be used as the template for 3D photonic crystals. The chain like phase 612 can be used to fabricate nanowire. The vortex ring 614 and chainlike 612 phases may be applied to electro-rheological fluids.

The growth of 3D colloidal crystals may be achieved in one example by growing 2D colloidal crystals in a layer-by-layer manner.

Example Strategy 1:

1) Choose concentration, zeta potential, size

a) In our given system, we use the Polystyrene microspheres, volume fraction = 0.2%, zeta potential=-26mv, size=1μm.

b) If changing the concentration of colloidal solution, the phase boundary will shift slightly.

c) The gap between two parallel glass electrode surfaces is fixed at 120μm. Therefore, E will be altered directly by changing the voltage.

2) Rough experiments to identify the ordered region

a) For a given voltage (such as Vp-p=2V), observe the pattern of the colloidal assembly by changing the frequency until an ordered phase appears.

b) Change voltage and frequency to identify the ordered phase domains.

3) Measurement of V-F phase diagram

a) Repeat the step 2 to identify the different phases and phase boundaries.

b) Cover the whole E-f (or V-f) regime by changing the voltage and frequency.

4) Identification of optimal "crystallization"

In the 2D ordered region, the change of voltage can affect the interaction between the particles, therefore change the lattice spacing; the change of frequency can affect the transport of particles, therefore control the local volume fraction of colloidal particles, therefore the nucleation rate of colloidal crystals. Under the certain conditions, we can achieve the high quality and large crystals by adjusting the voltage and frequency.

5) Growth of 2D crystals

We can prepare the same colloidal solution. According to the phase diagram, we can apply the optimum condition on the experimental cell. At a given voltage, we can adjust the frequency slightly to examine the quality of crystals. After these steps, we can get the high quality 2D colloidal crystals.

Theory

Nucleation is a dynamic process associated with overcoming a nucleation barrier. It occurs when small crystalline clusters form from structural when the liquid is in a state of supersaturation. The growth of these clusters depends on the competition between a decrease in bulk energy, which favours growth, and an increase in surface energy (line energy in 2D nucleation), which favours shrinkage. The smallest crystals are continually formed by fluctuations but then typically shrink away because of the high surface energy. Growth becomes energetically favourable only when the crystallites reach a critical size. According to the 2D

nucleation theory,8-10 the nucleation barrier that is the cost of the total (Gibbs) free-energy G_{crit} to form a critical circular nucleus with radius r_c in a supersaturated solution, is

$$\Delta G_{crit} = \frac{\pi\Omega\gamma^2}{\Delta\mu} \quad (1)$$

The critical size of the nucleus is

$$r_c = \frac{\Omega\gamma}{\Delta\mu} \quad (2)$$

where γ is the crystal-liquid interfacial edge free energy (or line tension), and is the volume per structural unit. Based on basic thermodynamic principles, μ for a given interparticle interaction can be expressed in terms of the supersaturation σ, as

$$\Delta\mu = k_B T \ln(1+\sigma) \quad (3)$$

Here the supersaturation is $\sigma = \frac{\varphi - \varphi_m}{\varphi_m}$; φ and φ_m represent the actual concentration and the equilibrium concentration of the colloidal spheres in the liquid phase, respectively.

In our experiments, the nucleation of charge-stabilized polystyrene (PS) spheres (diameter a = 0.99μm, polydispersity <5%, from Duke Scientific) in deionized water (resistance~18.2MΩ /cm) driven by an alternating electric field is examined quantitatively. The aqueous suspension of PS spheres (Volume fraction ϕ=0.2% and pH=4.34) is sandwiched and sealed in a glass cell composed of two pieces of conductive ITO glass (see experimental setup Fig. 1a). The zeta potential of the surface charge of the PS spheres is -26mV. The suspended PS spheres are uniformly dispersed in the water when the electric field is turned off. Once the alternating electric field is applied, the particles are transported to the surface of the electrode by the electric-field-induced fluid flow. Colloidal spheres were assembled in a 2D hexagonal close packing (hcp) formed at the bottom of the cell (see the inset of Fig.1a).

The driving force for the assembly of 2D crystals is determined by the interaction between the colloidal spheres and the local volume/area fraction of the colloidal spheres. In order to obtain a well defined supersaturation based on Eq.(3) in describing the nucleation kinetics, we examine the impact of Voltage Magnitude (V) and Voltage Frequency (f) of the applied AC field on the interparticle interaction and on the area fraction, that is the fraction of area covered by the colloidal particles on the surface of the electrode. The interparticle interaction is characterized by the position of the fist peak of the 2D pair correlation function (PCF) g(r). Fig.1b shows the variation of the position of the first peak of g(r) with increasing Voltage Magnitude. This implies that Voltage Magnitude (or the field strength E) will change

the interaction between the neighbouring particles. On the other hand, the position of the first peak of g(r) remains nearly the same (deviation <5%) at a constant Voltage Magnitude (cf. Fig.1c), meaning that the Voltage Frequency will not affect the interparticle interaction.

Nevertheless, a change of Voltage Frequency will result in a change of the transportation of the charged particles to the surface of electrode and alter the area/volume fraction of the colloidal particles (Fig.1d). According to Eq.(3) and Fig.1d, the driving force for the colloidal crystallization can be changed by altering . The dependence of the area fraction on the frequency is given in Fig.1d (keep V_{p-p}=2.4V). For a given system, 2D colloidal crystals approach the melt stage at f=3.0kHz, the area fraction of the colloidal particles corresponds to the area fraction at the equilibrium point φ_m(see the section on Methods for the details). Based on Fig. 1d, the concentration of the colloidal particles at the surface of the electrode can be controlled by altering the Voltage Frequency, which can be utilized to control the thermodynamic driving force as defined by Eq.(3). Therefore the disorder-order phase transition of 2D colloidal crystals can be controlled by changing the frequency of the AC field at a given voltage.

Experimental Results

Colloidal samples are in the liquid state (Volume fraction ϕ=0.2%) when no electric field is applied (see inset in Fig.1a). The particles were transported to the surface of electrode soon after applying an alternating electric field. A typical process of nucleation has been presented in Fig. 2. The concentration of the particles was supersaturated on the surface, and the particles started to form nuclei. This is shown in two early-time snapshots (Fig. 2a and b), where the crystal-like particles are highlighted by the blue spheres (see section on Methods: determination of crystal-like nuclei). The evolution of some nuclei is illustrated in these figures: the nuclei in the red circle kept on growing regardless of whether its state was pre- or post-nucleation; whereas the nuclei in the yellow circles shrank far more frequently than they grew (Fig. 2c-d).

Fig. 3a shows a typical distribution of various sizes of 2D crystalline clusters at different times (the voltage is V_{p-p}=2.4V , the field strength E=0.02V/m and the frequency is f=600Hz). As shown by Fig.3a, the distribution is initiated at curve 1 and gradually approaches curve 4, and is stabilized at curve 4. Actually the transition from curve 1 to curve 4 is a transition from a transient stable to a steady state of nucleation. In the context of nucleation, the critical size of nuclei is the size of the crystalline cluster which allows the crystalline clusters to grow

continuously at $n>n_c$ ($r>r_c$). We define $Z^*(t)$ to be the number of the largest crystalline cluster at a given time t, which should reach a constant value at $n>n_c$ ($r>r_c$) as shown in Fig.3a. The intercept between $Z(t)$ and $Z^*(t)$ gives rise to a critical cluster size $n^*(t)$ (see the inset in Fig. 3a). Fig. 3b shows that $n^*(t)$ increases with time and reaches a constant value at $t\geq\tau$. Obviously, τ is the induction time for the transition from the non-steady state to the steady state, and the constant value n_c is the critical nucleation size of a 2D nucleus at the steady nucleation state. Based on this principle, we can determine the critical size n_c and the critical radius r_c of a nucleus at different supersaturations (cf. Table I). The value of line tension γ is in good agreement with the simulation results ($\gamma_{line}\geq 0.43k_BT/a$) of a confined hard-sphere system.

The nucleation kinetics is characterized by a nucleation rate, which is defined as the number of "mature" nuclei ($r\geq r_c$) created per unit time-area. Following method illustrated in Figs. 3a and 3b allows us to examine this well defined state at a given supersaturation. According to the definition, the total number N of "mature" nuclei $n> n_c$ at a given area is plotted versus time t in Fig. 3c, which gives rise to a linear relation between N and t. The slope of the N versus t line corresponds to the steady nucleation rate. According to the 2D nucleation models, the nucleation rate of the steady state can be expressed as a function of supersaturation as

$$J = C\{\frac{2D_s n_1^2}{\pi}[\frac{\Omega \ln(1+\sigma)}{a}]^{1/2} \exp(-\frac{\pi\Omega a\gamma^2}{(k_BT)^2 \ln(1+\sigma)})\} \qquad (4)$$

Here D_s is the diffusion coefficient, n_1 is the number of single particles (monomers), C is the kinetic coefficient and a is the diameter of the colloidal particles. As shown in Fig.3d, a linear relationship between ln(J) and $1/\ln(1+\sigma)$ is attained, meaning that the steady state nucleation kinetics can be described very well by the current 2D nucleation theories. From this relationship, we can also get the average line tension at the interface, γ. The value of γ is $0.5k_BT/a$ which is in agreement with the average value ($\gamma\sim 0.47k_BT/a$) calculated from the Eq.(2) and shown in table 1 below.

Table I. The measured nucleation parameters at the various values of the driving force.

f (Hz)	φ (10^{-2})	μ (k_BT)	n_c	r_c (a)	γ (k_BT/a)	G_{crit} (k_BT)	J ($s^{-1}\mu m^{-2}$)
500	6.77	0.302	15±1.2	1.92	0.580	4.47	3.076±0.18
600	6.66	0.286	18±1.4	2.10	0.601	5.06	2.465±0.15
850	6.36	0.240	21±1.6	2.27	0.545	4.94	1.998±0.09

1000	6.16	0.208	26±1.4	2.56	0.532	5.41	1.599±0.09
1300	6.07	0.193	29±1.9	2.67	0.515	5.50	1.144±0.12
1700	5.74	0.150	32±1.7	2.83	0.425	4.82	0.871±0.07

The progress made in the understanding of the nucleation kinetics of colloidal crystals will allow us to identify a robust technology to produce large and high quality colloidal crystals. For instance, large and highly ordered colloidal crystals can be obtained at a low nucleation rate. In Fig.4, we compared 2D colloidal crystals produced at a constant and at an alternating electric field. When the electric field is constant, small and discrete crystallites are formed on the electrode. By applying an alternating electric field of frequency f, we are able to control the nucleation rate of the 2D colloidal crystals, so as to achieve a much better control of the level of perfection of the 2D crystals (involving a low density of defects, up to an area of $0.2x0.2mm^2$).

Experimental Methods

The Image recording setup is shown as Fig.1a. The in-situ continuous images are recorded by the digital imaging camera (Photometrics, CoolSNAP cf) which is mounted on an Olympus BX51 microscope. In the experiments reported here, we select the appropriate capturing rate (3.4 frames/second) and resolution ($1392x1040pixel^2$, corresponding to $258x193\mu m^2$ with the 50x and long working distance objective) to record the process of nucleation. Simultaneously the sequence of images is saved on a hard disc having large volume (120GB) by the image processing software. Based on these real-space images, we can identify the individual colloidal spheres and analyze the continuous process of pre- and post- nucleation.

Identification of crystal-like nuclei

We used two criteria to identify the crystal-like nuclei in the process of nucleation.

I) Define the neighboring between the particles: two particles were defined as neighbors if the centre to centre distance between the particles was smaller than a cutoff value of 1.80a (where a is the average diameter of the PS spheres), chosen to be close to the minimum between the first and second peaks of the pair correlation function g(r) for our samples, as shown in Fig.1c.

II) Identify the crystal-like nuclei: a particle was defined as a member of a 2D crystal if one particle had more than two neighbors. To exclude the structures of circles or dumbbell (two crystals linked with a long chain) and consider the structural relaxation, we further confined the bond angles between a particle and its neighbors to $\pi/3\pm\pi/12$. We used these two criteria to

identify the crystal-like nuclei during the nucleation of colloidal particles.

Measurement of the supersaturation

The transport of particles was controlled by the fluid flow induced by the alternating electric field. In our observation, the fluid flow was a function of the frequency. In Fig. 1d shows a plot of the concentration of the particles which arrived at the surface of the electrode in terms of the fraction of the occupied area against the frequency of applied field. To measure the supersaturation accurately, we used the ultrasonic (with the duration of 10 minutes) to redisperse the colloidal particles each time before re-applying the alternating electric field. When the concentration on the surface caused the area of the electrode to be fully supersaturated, the nuclei appeared and formed. We considered that moment to make the onset of supersaturation, and we measured the concentration of the particles on the surface at that instant. When we increased the frequency of the electric filed to 3kHz, we noticed that the colloidal crystals were starting to melt, and we measured simultaneously the concentration of the liquid-like particles around the crystallites at the equilibrium point φ_m (Fig. 1d).

Phase Behaviour

The external fields, such as electric and magnetic fields, gravity, structured or confining walls and shear, can guide and manipulate the self-organization of the colloidal particles in desired directions. Moreover, the controls of the colloidal systems involving electric fields are especially popular topics of research. Despite nearly two decades of study, the response of charged particles dispersed in water to the influence of electric fields remains a mystery and is opposite to what is expected from electrostatic considerations, especially in cases when the particles also interact strongly with each other. For example, alternating electric fields (AEF) have been found to organize colloidal dispersions into such complex configurations as circulating chevron bands oblique to the field, vortex rings perpendicular to the field, super lattice structures in the binary system, and even colloidal crystals. In particular, particles driven by electric fields onto the surface of an electrode develop long-range in-plane attractions strong enough to induce two-dimensional (2D) crystallization. It was suggested by Trau et al. (Trau, M., Saville, D. A. & Aksay, I. A. *Science* 272, 706–709 (1996), and M. Trau, D. A. Saville, I. A. Aksay, *Langmuir* 13, 6375 (1997)) that these effects result from field-induced electrohydrodynamic forces. Due to the fact that colloidal spheres reveal similar phase behaviors as small molecular systems, and they are visible microscopely, they have been chosen as model systems for investigating fundamental questions related phase

transition, such as crystallization and melting. To date, no systematic and detailed study has been performed on the pattern formation and the phase behavior induced by an AEF in a monodisperse charge-stabilized colloidal suspension.

The present invention allows the first measurement of the phase diagram of colloidal patterns obtained by varying the field strength σ_E and frequency f of a vertical AEF. In mapping out different conditions, a wide range of patterns such as oscillatory interlinked chains, oscillatory vortex ring, three-dimensional (3D) aggregation and crystalline monolayer are generated by an alternating electric field. Furthermore, the new critical phase behaviour of the order-disorder phase transitions in the colloidal systems is observed and a direct imaging of such a transition is made.

a) Experimental

In one example the present invention employs a suspension of monodisperse colloidal polystyrene (PS) spheres (Diameter $d = 1.0 \mu m$, Duck Scientific) which is confined to a horizontal layer between two conductive glass microscope slides. The edges of this sample holder are sealed with a UV cured adhesive (Norland Industries, Type 88) to prevent evaporation of the water from the suspension. Glass spacers set the layer thickness in the cells at $H = 120 \pm 5 \mu m$ across the $1.5 \times 1.5 cm^2$ observation area. The bulk volume fraction of spheres in suspension is 0.2%. The suspension equilibrates in air at a pH of roughly 4.7. The surfaces of both the lower and the upper glass coverslips are coated with a thin layer of Indium Titanium Oxide (ITO, ~100nm), while they are still optically thin and allows for the application of uniform vertical electric fields to the confined suspension. This simple setup gives rise to a complicated coupling among hydrodynamic flows and reaction-diffusion of ions and colloidal particles in the electric field. The sample cell is mounted on an optical microscope (Olympus BX51) so that the motions of colloidal particles can be recorded with a digital CCD camera connected to a computer. Considering that the density ρ of colloidal polystyrene is very close to the water ($\Delta\rho = 0.05 g/ml$) and the zeta potential φ_z of negatively charged spheres is $-26 \pm 1.6 mV$, such spheres can disperse uniformly in the water in the absence of an electric field when the volume fraction of the suspension is not too high. The patterns of colloidal assembly on both the top and bottom surfaces of the electrodes and in the bulk occur when an AEF is applied.

A detailed $\sigma_E \sim f$ phase diagram of colloidal suspensions from a 2D crystal, a 3D

aggregation, oscillating vortex rings and chains is given in Figure 6 and its insets. At a low field strength ($\sigma_E < 0.9\times10^4 V/m$), the response of the colloidal spheres is quite slow, and insensitive to the field (not shown in the figure). While the frequency changes, the phase is in the liquid state as shown at 604. The transition to dynamical patterns occurs at a field strength σ_E exceeding$1\times10^4 V/m$, thus the regions involving chains, oscillating vortex rings, three-dimensional aggregation and the ordered colloidal monolayer occur subsequently within different frequency domains.

Reference 606 is a 2D colloidal crystal on the surface of the electrodes under an applied electric field ($\sigma_E = 2.6\times10^4 V/m, f = 600Hz$). The spheres will nucleate and grow to two-dimensional highly-ordered colloidal crystals when the appropriate AEF is applied; while in reference 616, the disordered 3D aggregation of particles is formed under an electric field of lower frequency ($\sigma_E = 2.4\times10^4 V/m, f = 100Hz$). The interior of the aggregation region is invisible under the optical microscope. The patterns shown in references 606 and 616 are stationary unlike references 612 and 614. Additionally, we used the laser confocal microscope (Leica TCS SP2) to visualize the interior structure of the aggregation by fluorescent dyed spheres of polystyrene (Bang Laboratories, FS04F). The size and zeta potential ($d = 1.02\mu m, \varphi_Z = -35 \pm 2.1mV$) of this suspension are similar with the plain PS suspension we used.

Reference 612 shows a typical pattern of vortex rings bounded by a rapidly circulating toroid whose spheres travel downward along the inner surface and return upward along the exterior, completing one cycle in a few seconds. At the same time the whole toroid is oscillating with the frequency of the applied electric field. Reference 614 shows typical tangled chains composed of colloidal spheres when a low-frequency electric field is applied ($\sigma_E = 1.8\times10^4 V/m, f = 0.1Hz$). These chains form the interlinked mesh in the bulk of the suspension and oscillate with the frequency of the external field.

A strength-dependent phase transition from the liquid state to the crystalline monolayer occurs at a constant frequency f as the strength σ_E increases (the cross dot in Figure 6). To characterize this phase transition, the translational correlation function $g(r)$ and bond-orientational correlation function $g_6(r)$ were computed from the data of the central-mass positions of the particles, as determined by the digitized and processed images. Figures 7A and B show the plots of $g(r)$ and $g_6(r)$ as functions of strength σ_E. A dramatic change of the

translational order and angular order is observed as the strength σ_E decreases gradually. As the phase points move down along the cross dot in the phase diagram, the peaks of $g(r)$ become discrete and smoothened off, converging to 1. Meanwhile the curve of $g_6(r)$ decays rapidly from 1 to 0. The $g(r)$ and $g_6(r)$ functions of computer-generated hexagonal lattices are displayed in Figure 7 $g(r)$ is composed of the discrete delta peaks at certain distances r and approaches 1 at the infinite distance. $g_6(r)$ comprises discrete constants (equal to 1) at certain distances. Then a random translation in both the x and y directions was induced based on the computer-generated lattices. Whenever the induced random translation was less than 10%, the $g(r)$ and $g_6(r)$ functions coincided with the corresponding functions referring to the experimental curve of $\sigma_E = 2.6\times10^4 V/m$. It turns out that the perfection of the crystalline monolayer of colloids in our experiments is very close to the perfect 2D hexagonal lattices.

This phase behaviour can be further described by the order parameters, the translational correlation length ξ_T and the power-law exponent η_6 which reflect the exponential decay of $g(r)$: e^{-r/ξ_T} and the power-law decay of $g_6(r)$: $r^{-\eta_6}$. As shown in Figure 8a, the translational correlation length ξ_T changes from $1.5a$ (a is the particle diameter) to $15.3a$ when the field strength increases gradually, meaning that the translation gains a long range order (the translational correlation length of the computer-generated lattices is around $40a$). Simultaneously, the values of decay exponents η_6 decrease from 0.56 to zero as shown in Figure 8b. As shown in the phase diagram (Figure 6), the disorder-order phase transition occurs on the phase boundary of the 2D colloidal crystals.

b) Theory

In the Kosterlitz-Thouless-Halperin-Nelson-Young (KTHNY) theory for 2D crystal melting, three different phases are distinguished from one another by the characteristic behavior of their translational and bond-orientational orders. As the KTHNY theory predicted, the crystalline phase is characterized by a long-range orientational order and a quasi-long-range translational order. In the isotropic fluid phase, both the orientational and translational orders are short ranged. The intermediate hexatic phase is characterized by a quasi-long-range orientational order and a short-range translational order. In the KTHNY theory, the disorder-order phase transition of a colloidal system is widely believed to be a second-order transition. It is surprising to see that in our system, the first derivative of the correlation length changes

continuously at the critical field strength. Therefore the phase transition is of a much higher order than a second order.

To investigate the order of the transition occurring in our system, the order parameters were rescaled by the values of order parameters ξ_T and η_6 of the liquid and solid state in our experiments. The ln-ln plots of the rescaled order parameters ξ_T' and η_6' against the critical field strength are shown in Fig. 9. Both of the plots, $\ln(-\ln(\xi_T'))$ and $\ln[-\ln(\eta_6')] \sim \ln(\sigma_E - \sigma_E^c)$, appear to fall on a straight line as the critical point σ_E^c is approached, indicating that the rescaled order parameters ξ_T' and η_6' can be well approximated by a function $e^{-\alpha(\sigma_E-\sigma_E^c)^\beta}$ (α, β are the fitting parameters, $\alpha > 0$ and $\beta < 0$). The functional form of the order parameters implies that the phase transition is in fact of infinite order, since all derivatives of the order parameters vanish at the critical point σ_E^c. Furthermore, in Figs. 8A and B, the experimental data of the order parameters can be fit very well by the above exponential function with the given fitting parameters. Such an infinite-order type or Kosterlitz-Thouless type of order-disorder phase transition has never been observed in real systems before.

The richness of the phases and phase behaviours of colloidal assembly controlled by an AEF has given rise to interesting fundamental questions of condensed matter. The remarkable and unexpected results of the investigation of the field-strength-dependent phase transition in the colloidal system presents a real model system for the infinite-order phase transition, which is only predicted by the theoretical models or simulations. The present system significantly extends the use of colloids as condensed matter model systems. At the mean time, the different colloidal phases with the control of external fields are being used in the realization of new materials. Here we can expect that the rich colloidal patterns that can be produced by achieving an increased manipulation by the external field will lead to important extensions of model systems for condensed matter and creation of new functional materials.

Phase Transitions

The solid-liquid phase transition is one of the fundamental topics in condensed matter physics. Its study has received new impulses since phase transitions can be observed on a microscopic level by accompanying the development of direct imaging in model system of colloids. Unlike the atoms in conventional materials, the individual spheres can be imaged with a conventional light microscope on time scales compatible with standard video equipment and microscopic structure and dynamics of colloidal suspensions can be studied with

"atomic" resolution. The frontiers investigated the phase transitions of 2D colloidal system and found qualitative consistency with a two-step melting transition through a hexatic phase, which still exhibits quasi-long-range orientational order but only short-range translational order. This result falls in the predication of the Kosterlitz-Thouless-Halperin-Nelson-Young (KTHNY) theory. But there are still some open questions between the experiments and KTHNY's predication, such as the order of the phase transitions and scaling of the correlations. Over the past decade, the various experiments on the 2D melting or phase transitions in the different colloidal systems were reported. Among these results, there is an active debate of the existence of hexatic phase, and if the hexatic phase exists whether the transitions are first order or continuous.

To date, both experimental and computer simulation studies of 2D melting have focused attention, almost exclusively, on the search for continuous transition from the solid to the hexatic phase and from the hexatic phase to the liquid phase. However it appears no previous experiments or simulations have been carried out to observe the disorder-order phase transitions in the 2D colloidal system induced by an alternating electric field. The experiments below demonstrate that the observations of two scenarios of the colloidal phase transitions which have the different characters of phase transitions, one is the infinite order and the other is the second order.

a) Experimental

In one example the present invention will present an experimental system consisting of monodisperse polystyrene particles with a diameter of $0.99\,\mu m$ and a mass density of $1.05 g/cm^3$ (Bangs Laboratory) which are sandwiched by the two conductive glass slides. As shown in Figure 1a, an alternating electric field generated by a waveform generator (Agilent, 33120A) is applied on the flat electrodes along the Z direction. The glass sample cell is clamped on the microscope (Olympus BX51). Consistently reproducible images are recorded into a computer by a digital CCD camera (CoolSNAP cf) over 30 minutes for each equilibrium-established sample. The different patterns of colloidal assembly change with the field strength and frequency respectively. The complete phase diagram of colloidal phases induced by an alternating electric field has been summarized in our manuscript. In this letter we will focus on the disorder-order phase transitions during the crystallization of colloidal monolayer. As shown in Figure 10, there are two kind of phase transitions can be observed, one is the strength-dependent phase transition (the series of dots 101) and the other is the frequency-dependent

phase transition (the series of squares 103).

In order to characterize the observed phase transitions, we use the pair correlation function $g(r)$ and the bond-orientational correlation function $g_6(r)$, which are respectively defined as:

$$g(r) = \langle \rho_G(0)\rho_G(r) \rangle, \quad \rho_G(r) = \sum_{i=1}^{N} e^{iG \cdot r_i} \delta(r - r_i) \tag{1}$$

$$g_6(r) = \frac{\langle \psi_6^*(0)\psi_6(r) \rangle}{\langle \delta(r_i)\delta(r_j - r) \rangle}, \quad \psi_6(r_i) = \langle \frac{1}{N} \sum_j e^{6i\theta(r_{ij})} \rangle \tag{2}$$

G denotes a reciprocal-lattice vector of the solid, and $\theta(r_{ij})$ is the angle between the bond connecting particles i and j and an arbitrary fixed reference axis. Furthermore, the translational order parameter ξ_T and bond-orientational order parameter η_6 are defined respectively. ξ_T is the correlation length which are defined the exponentially-decayed exponents of $g(r)$: e^{-r/ξ_T}, and similarly η_6 is the characteristic exponents of power-law-decayed $g_6(r)$: $r^{-\eta_6}$. For the ordered 2D lattice, the translational correlation length ξ_T of $g(r)$ is quite large ($\sim 40a$) and bond-orientational order η_6 is a near-zero value; for the isotropic liquid, ξ_T is close to a and η_6 is larger than 0.25. Here, a is the lattice spacing.

The results reported herein were observed for two typical scenarios of phase transitions, one induced by the field strength between $3\times10^4 V/m$ and 0 with a fixed frequency $f = 0.8kHz$ and the other induced by the frequency between $0.8kHz$ and $4.5kHz$ with a fixed strength ($\sigma_E = 2.8\times10^4 V/m$). In this region we find the disorder-order phase transitions, which evolve from the isotropic fluid to 2D colloidal crystals when we increase the field strength or decrease the frequency respectively. This is illustrated in Figure 10, which shows that there is a broad phase boundary between the solid state and isotropic fluid. That means the transition of disorder to order will experience the intermediate phases. The translational correlation length ξ_T and bond-orientational exponent η_6 are chosen as the order parameter to characterize these phase transitions and determine the phase boundaries. As shown in Figure 11a, the correlation length ξ_T and bond-orientational order η_6 reflect exactly that phase behavior induced by the field strength. ξ_T (Bottom of Figure 11a) changes from the shortest range a to long range $14a$. When the field strength reaches a critical value $\sigma_E^c = 0.9\times10^4 V/m$, ξ_T starts to increase; after the field strength passes the value $2.8\times10^4 V/m$, ξ_T is close to the value

of solid state. Whereas the bond-orientational order η_6 (Top of Figure 11a) also follows the same behaviours. Therefore the phase boundary at the fixed frequency ($f = 0.8kHz$) can be determined by mapping the variation of order parameters. Figure 11b shows the order parameters of the frequency-dependent phase behaviour at the fixed strength $\sigma_E = 2.8\times10^4 V/m$. Accordingly, the critical frequency f_c and phase boundaries can be determined. With the similar measurement at the different strength and frequency, the complete phase boundaries of disorder-order phase transition can be determined. However, the transition induced by the frequency is much abrupt than the strength-dependent transition. Compare with the Figures 11a and b, the relative transition window of frequency-dependent transition is narrower than the strength-dependent transition.

b) Theory

The classical Landau-Ginzburg theory of phase transition classifies the phase transitions according to the order of phase transitions. The order of phase transitions gives us the concept of classification of phase transitions and the critical behaviour of order parameters approaching the critical conditions. To investigate the order of the transition in our experiments, the log plot of correlation length versus the critical field strength is shown in Figure 12a which suggests the order parameter approaches zero faster than a power law as σ_E approaches the critical point. Furthermore, the plot of $\ln[-\ln(\xi_T)] \sim \ln(\sigma_E - \sigma_E^C)$ appears to fall on a straight line as approaching the critical point, indicating that the correlation length can be well approximated by a function $\xi_T \sim e^{-\alpha(\sigma_E-\sigma_E^c)^\beta}$ ($\sigma \to \sigma_C$). This implies that the phase transition is in fact of infinite order, since all derivatives vanish at the critical point. Such an infinite-order type or Kosterlitz-Thouless type of order-disorder phase has never been observed before.

The observation of an infinite-order phase transition induced by the strength σ_E of an alternating electric field is rather surprising. These columns are oriented parallel to the in-plane component of the magnetic field leading to long-range orientational order. They are well separated from each other, and quasi-long-range translational order is observed perpendicular to these columns. However, along these columns particles can easily move and their trajectories overlap. Consequently the Lindemann parameter in this direction diverges and translational order is short range parallel to the field.

Furthermore, the plot of $\ln(\xi_T/a)$: $\ln(f - f_c)$ is fit by a straight line as shown in Figure

12b. Accordingly, the correlation length can be expressed as a function $\xi_T / a : (f - f_c)^{\beta}$ as $f \to f_c$. In particular, the linear fitting parameter β is exactly equal to 2.09 ± 0.03 indicating that the appropriate asymptotic form for ξ_T is $\xi_T / a : (f - f_c)^2$. The first order derivative of the function of the correlation length $\xi_T(f)$ is still continuous. That means the frequency-dependent phase transition is a second-order phase transition.

In our experimental system, the strength and frequency of an alternating electric field can induce two different phase behaviours which have the different characters. The essential physics in these phase behaviours is a subtle difference of interaction between the colloidal particles. When decreasing the strength with a fixed frequency, the crystalline monolayer starts to expand and simultaneously the coordinates of particles are distorted compared to the highly-ordered lattice. As shown in Figure 13, the lattice spacing of the 2D crystallites (circle dots) increases and expands to 25% than the most compact lattice before transferring to the isotropic liquid. Alternatively, when increasing the frequency with a fixed strength, the 2D crystallites keep their lattice until the frequency arrive a critical value. After that, the lattice will dismiss and return to disorder state quickly. As shown by the square dots in Figure 13, the lattice spacing remains constant throughout the range of frequency.

Several experiments suggest that the dipole-dipole interactions can produce the planar close-packed arrays in the colloidal system. The external electric field will polarize the colloidal particles and their double layers since the polystyrene particles and water are insulate. Therefore, one point dipole moment can be expressed as

$$\vec{P} = \alpha(f)\vec{\sigma}_{loc}, \qquad (3)$$

$\vec{\sigma}_{loc}$ is the local field strength exerting on the particle, $\vec{\sigma}_{loc} = (\varepsilon_w / \varepsilon_s)\vec{\sigma}_E$ (ε_w and ε_s are the dielectric constant of the water and sphere, respectively. $\vec{\sigma}_E$ is an uniform external field strength along z direction.). $\alpha(f)$ is the polarizability of the sphere and can be expressed as:

$$\alpha(f) = \frac{\alpha_0}{1 - (f / f_0)^2}, \qquad (4)$$

α_0 and f_0 are the static polarizability and eigenfrequency respectively. The dipole-dipole interaction between the pair of particles can be given by

$$U_{ij} = \frac{\vec{P}_i \cdot \vec{P}_j}{r^3}, \qquad (5)$$

r is the interparticle distance between the sphere i and j. Here only the first order

approximation of the interaction is presented. Because of the polydisperse distribution of the spheres, the eigenfrequency of the spheres should have a range of distribution Δf_0. Note that the polarizability is a nonmonotonic function of frequency. When the frequency of external field is out of range of the eigenfrequency, the dipole moment $\vec{P}$ has the same sign. According to Eqs. (3)-(5), the interaction is repulsive ($U_{ij} > 0$). Contrarily when the external frequency f falls in the range of eigenfrequency, the direction of $\vec{P}_i$ and $\vec{P}_j$ is inverse and the interaction is attractive ($U_{ij} < 0$). Above prediction is consistent with our experimental observation of the frequency-dependent phase transition. The increasing frequency makes the dipole-dipole interaction undergo a transition form the attraction to repulsion. On the other hand, the field strength σ_E merely affects the amplitude of the interaction according to Eqs (3) and (5). At certain frequency ($f = 800Hz$), the decreasing field strength lowers the attractive interaction until the attractive interaction is very low and fail to resist the random Brownian motion of the colloidal particles. Above scenario describes the strength-dependent phase transition. In another word, the different characteristics of the interaction in two scenarios of phase transitions result in the different critical behaviours with the difference of order of phase transition.

Described above are two scenarios of colloidal phase transitions induced by the field strength and frequency of an alternating electric field respectively. It is surprising that the strength-dependent phase transition is an infinite-order phase transition, whereas the frequency-dependent phase transition is a second-order phase transition. This very intriguing fact may be induced by the subtle competition of two parameters of external electric field. This experimental accessibility coupled with their rich and varied phase behaviour set colloidal suspensions apart as an unusually powerful class of model systems for studying the microscopic processes underlying structural phase transitions.

According to the experiments, the methods of the present can produce particle sizes from 200nm to $5\,\mu m$. As shown in figures 14a and 14b, the 2D colloidal crystals can be obtained with the particles of 200nm and $5\,\mu m$. While this is the range produced experimentally, it is not to limit the range of particle sizes produced by the method of the invention. It is envisioned that the present invention may be employed for the nano scale assembly of colloidal particles.

In Figure 5 we see that at the isoelectric point (where the colloidal particles are nearly neutral), the particles only form the short chains under an alternating electric field.

The different particle sizes correspond to the different optimum frequencies when the 2D crystals are formed (see the table below).

Particle size	Optimum Frequency
5 μm	~60Hz
1.68 μm	~300Hz
1.0 μm	~800Hz
200nm	~1500Hz

The value of zeta potential represents the density of the surface charge of the particles (the sign of zeta potential corresponds to the sign of charge of particles). The zeta potential can be changed by altering the pH or the ionic strength of the suspension. The titration curve and the pattern of neutral particles are presented in Figure 15. It appears that lower zeta potentials can not facilitate the assembly of 2D colloidal crystals, and the sign of the zeta potential has no affect on the experimental results. At the isoelectric point the value of zeta potential equals to zero at certain pH value. From the curve in Figure 15, we can see the zeta potential can change from the positive to negative.

Alternative embodiments

The prior art is restricted to monodisperse and binary mixtures, whereas the present method is applicable to mondisperse mixtures of particles. It is also possible to extend the present invention to binary as well as polydisperse mixtures.

The prior art utilizes flat surfaces that are parallel or inclined at an angle, i.e. the flat surfaces need not be parallel, whereas the present invention provides for an improved method of preparing an improved end-product on flat surfaces. It is possible to extend the present invention to non-parallel flat surfaces.

It is additionally possible to control the shape of the surface by extending the present invention to curved surfaces, that may be concave or convex. Nowhere in the prior art are curved surfaces introduced, whereas, the present invention is applicable for curved surfaces

applications for which flat surfaces are inappropriate.

Finally, the present invention provides a way of controlling the symmetry properties of the two-dimensional structure. By changing the wave form at low concentrations and at low frequencies (<100Hz), we are able to trigger a transformation of the end-product from one pattern to a different pattern. Again, this feature has thus far not been entertained in the prior art.

CLAIMS

1. A method of identifying optimum electric field conditions for forming a colloidal structure from particles within a solution comprising the steps of:

applying an AC electric field to the solution and varying the frequency;

applying an AC electric field to the solution and varying the magnitude; and

identifying an optimum range of frequencies and magnitudes to form said colloidal structure.

2. A method as claimed in claim 1 wherein said optimum range is at least partially bounded by at least one phase transition.

3. A method as claimed in claim 2 wherein the optimum range of magnitude is bounded by an infinite order phase transition.

4. A method as claimed in claim 3 wherein the optimum range of frequency is bounded by one or more second order phase transitions.

5. A method as claimed in claims 1 to 4 wherein said optimum range is characterised by a particle spacing less than a predetermined threshold.

6. A method as claimed in claims 5 wherein said optimum range is characterised by more than two particles spaced less than a predetermined threshold from one another.

7. A method as claimed in claim 6 wherein said optimum range is further characterised by a particle to particle bond angle within a predetermined range.

8. A method as claimed in any one of claims 1 to 7 wherein said optimum range is characterised by said particles not being fluid or disordered.

9. A method as claimed in any one of claims 1 to 8 wherein said optimum range is characterised by said particles not being unstable or where the electric field is so high that chemical reaction occur.

10. A method as claimed in any one of claims 1 to 9 further comprising the step of identifying the boundaries between ideally formed and non ideally formed structures.

11. A method as claimed in claim 10 further comprising the step of identifying the type or order of said phase transitions.

12. A method as claimed in claim 11 wherein said type or order are characterised by determining the pair correlation function $g(r)$ and the bond-orientational correlation function $g_6(r)$ from the respective equations:

$$g(r) = \langle \rho_G(0)\rho_G(r) \rangle, \quad \rho_G(r) = \sum_{i=1}^{N} e^{iG \cdot r_i} \delta(r - r_i)$$

$$g_6(r) = \frac{\langle \psi_6^*(0)\psi_6(r) \rangle}{\langle \delta(r_i)\delta(r_j - r) \rangle}, \quad \psi_6(r_i) = \langle \frac{1}{N} \sum_j e^{6i\theta(r_{ij})} \rangle$$

wherein G denotes a reciprocal-lattice vector of a solid, and $\theta(r_{ij})$ is the angle between the bond connecting particles i and j and an arbitrary fixed reference axis.

13. A method as claimed in claim 11 wherein said type or order are determined by approximating a ln plot of the order parameters order parameters of the translational correlation length ξ_T and the power-law exponent η_6 with the function $e^{-\alpha(\sigma_E - \sigma_E^C)^\beta}$, wherein α, β are the fitting parameters.

14. A method as claimed in any one of claims 1 to 13 wherein said optimum range is further comprised of a oscillating chain-like phase.

15. A method as claimed in any one of claims 1 to 14 wherein said optimum range is further comprised of a vortex ring phase.

16. A method as claimed in any one of claims 1 to 15 wherein said optimum range is further comprised of a 3D aggregation phase.

17. A method as claimed in any one of claims 1 to 16 wherein said optimum range is further comprised of a 2D hexagonal close packed phase.

18. A method or process of preparing a substantially crystalline colloidal structure (colloidal crystal) between electrodes comprising or including the steps of:

selecting a colloid system from which the colloidal crystal will be formed;

selecting a electrode AC voltage magnitude and frequency from a preferred domain of magnitude against frequency which gives rise to a substantially stable colloidal crystal; and

providing an electric field from said electrodes using said selection to prepare the colloidal crystal, which may be in substantially two dimensions or substantially in three dimensions, on or proximal to the surface of one electrode.

19. A method as claimed in claim 18 wherein said preferred domain of electrode potential against frequency is compiled by conducting at least three experiments/runs of measuring electrode potential against frequency wherein there are at least two different potentials applied/used/measured and there are at least two different frequencies applied/used/measured.

20. A method as claimed in claim 18 wherein said preferred domain of electrode potential against frequency is compiled according to any one of claims 1 to 17.

21. A method as claimed in any one of claims 18 to 20 wherein the step of generally identifying the domain of electrode potential against frequency includes using the results of the at least three experiments/runs to prepare (whether very generally or in detail) a phase diagram showing (whether very generally or very accurately) regions of ordered and disordered colloidal behavior.

22. A method as claimed in any one of claims 18 to 21 wherein the step of preparing the phase diagram involves observing the pattern of the colloidal assembly with each experiment /run.

23. A method as claimed in any one of claims 18 to 22 wherein the at least three experiments/runs are obtained by the acts of (in no particular order):

holding the AC voltage magnitude substantially constant, varying the frequency

and observing the pattern of the colloidal assembly at least once; and

holding the AC voltage frequency substantially constant, varying the voltage and observing the pattern of the colloidal assembly at least once.

24. A method as claimed in any one of claims 18 to 23 wherein the step of generally identifying said domain of electrode potential against frequency includes using the results of the at least three experiments/runs to prepare (whether very generally or in detail) a phase diagram showing (whether very generally or very accurately) one or more of:

a domain of oscillating chain like behavior of the colloid system;

a domain of vortex ring behavior of the colloid system;

a domain of three dimensional colloidal aggregation, between the electrodes, within the colloid system;

a domain of disordered behavior of the colloid system;

a domain of hexagonally close packed two dimensional formation of a colloidal crystal, between the electrodes, within the colloid system; and

a domain of instability or of the solution chemically reacting.

25. A method as claimed in any one of claims 18 to 24 wherein the colloidal crystal may be substantially planar (in two dimensions).

26. A method as claimed in any one of claims 18 to 24 wherein the colloidal crystal may be in three dimensions.

27. A method as claimed in any one of claims 18 to 24 wherein the colloidal crystal may be a mixture of two and three dimension.

28. A method as claimed in any one of claims 18 to 27 wherein the step of selecting the colloid system includes selecting the solvent, concentration, pH, and diameter of colloidal spheres.

29. A method as claimed in any one of claims 18 to 28 wherein the step of preparing the phase diagram involves one or more of:

knowledge of the distance of separation between the electrodes;

knowledge of the volume fraction of the colloids;
knowledge of the zeta potential of the colloids; and
knowledge of the size of the colloids.

30. A method as claimed in claims 18 to 29 wherein the diameter of colloidal crystals is at least 100μm.

31. A colloidal crystal prepared substantially according to the method or process as claimed in any one of claims 18 to 30.

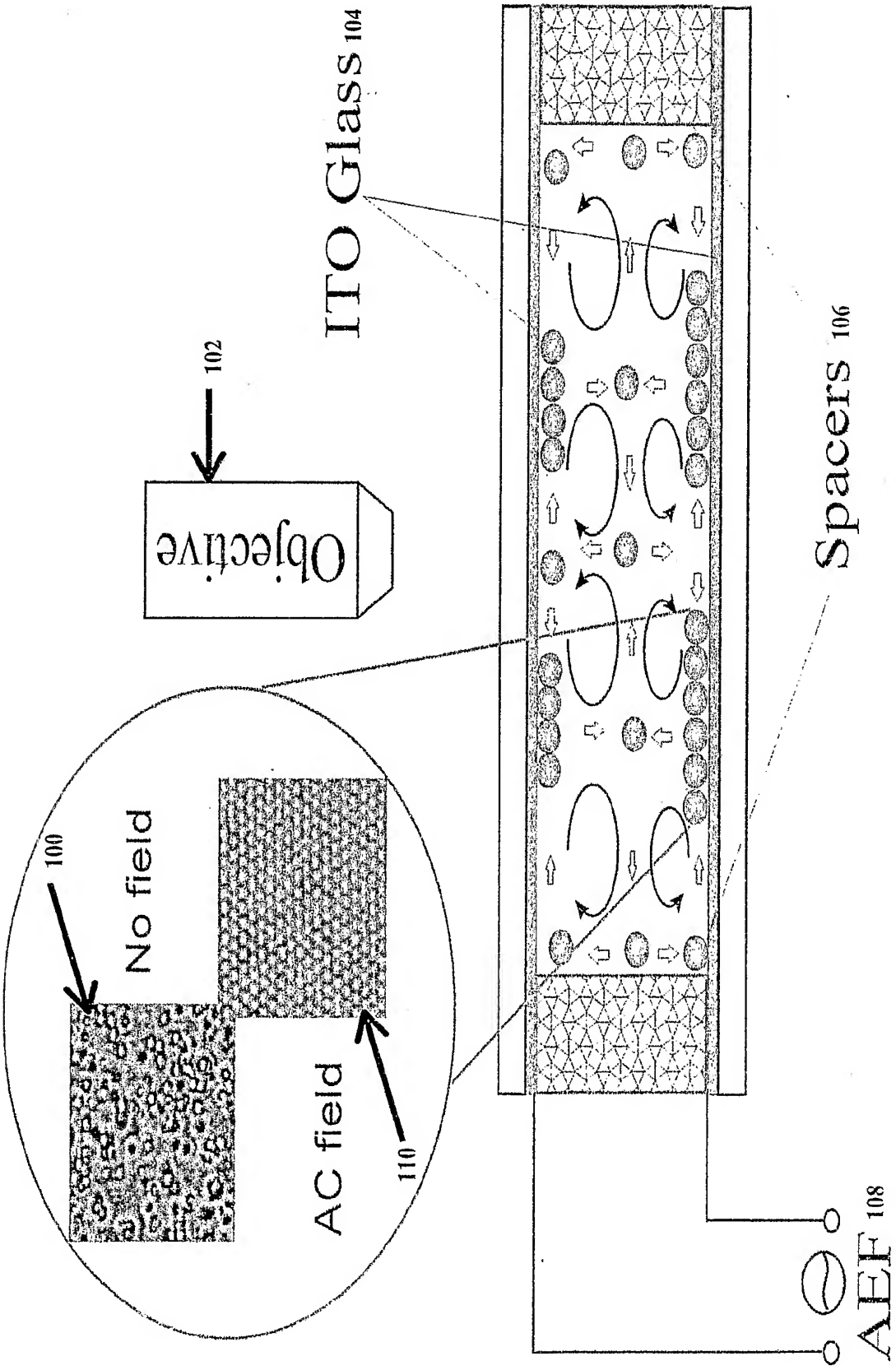
ITO Glass 104
102
Objective
Spacers 106
100
No field
AC field
110
AEF 108

FIGURE 1a

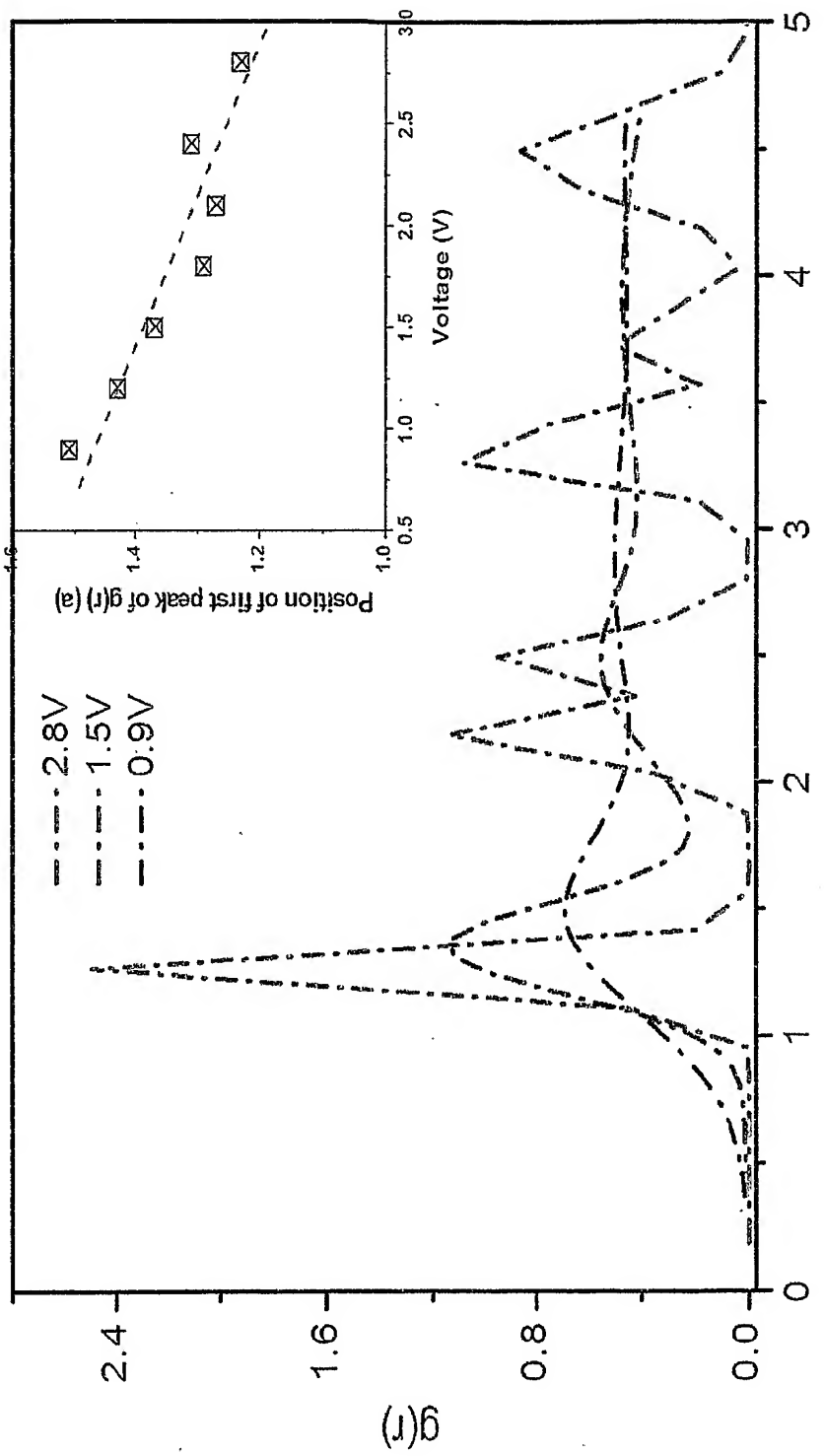

FIGURE 1b

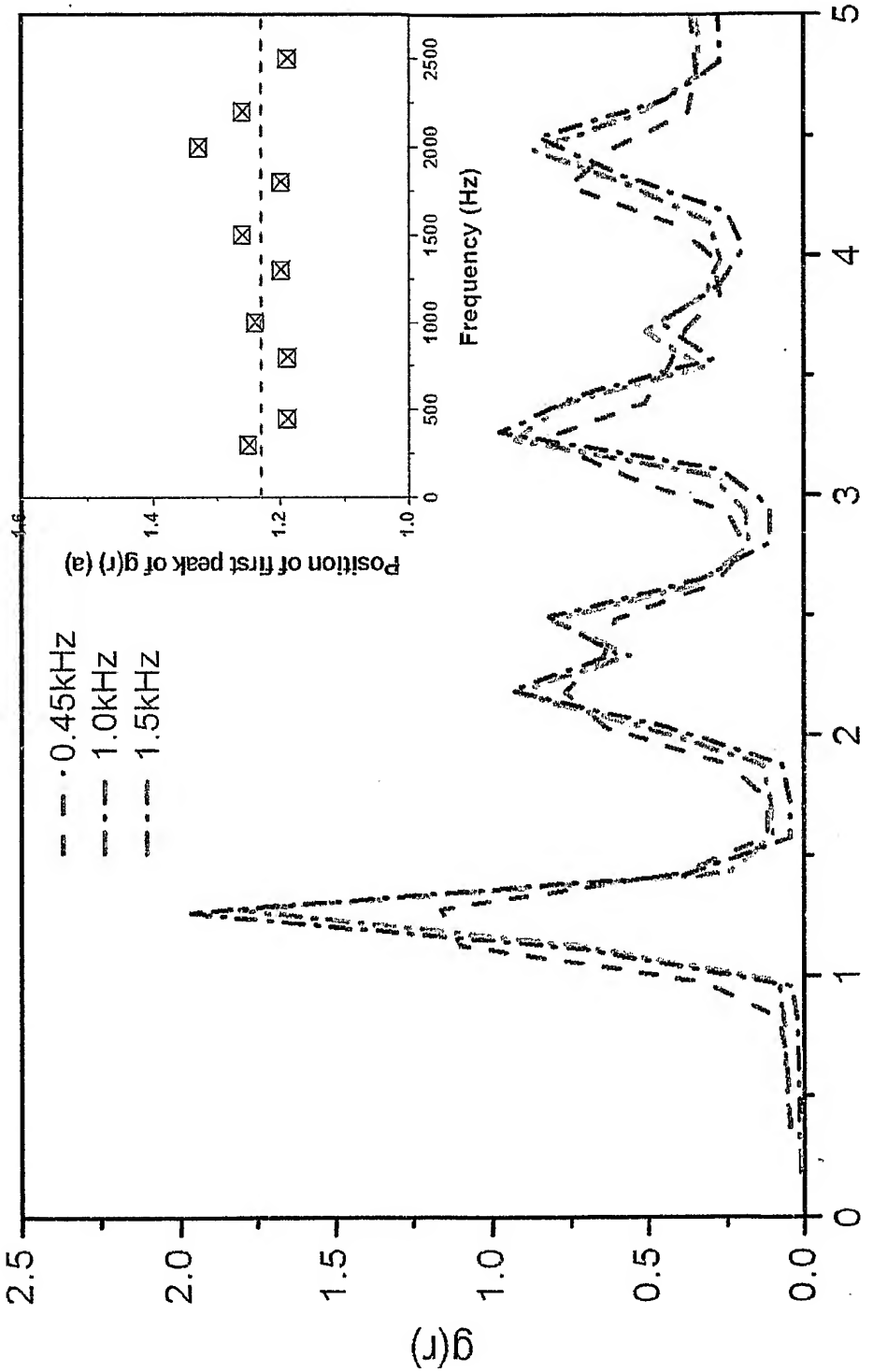
g(r)
r/a
0.45kHz
1.0kHz
1.5kHz
Position of first peak of g(r) (a)
Frequency (Hz)

FIGURE 1c

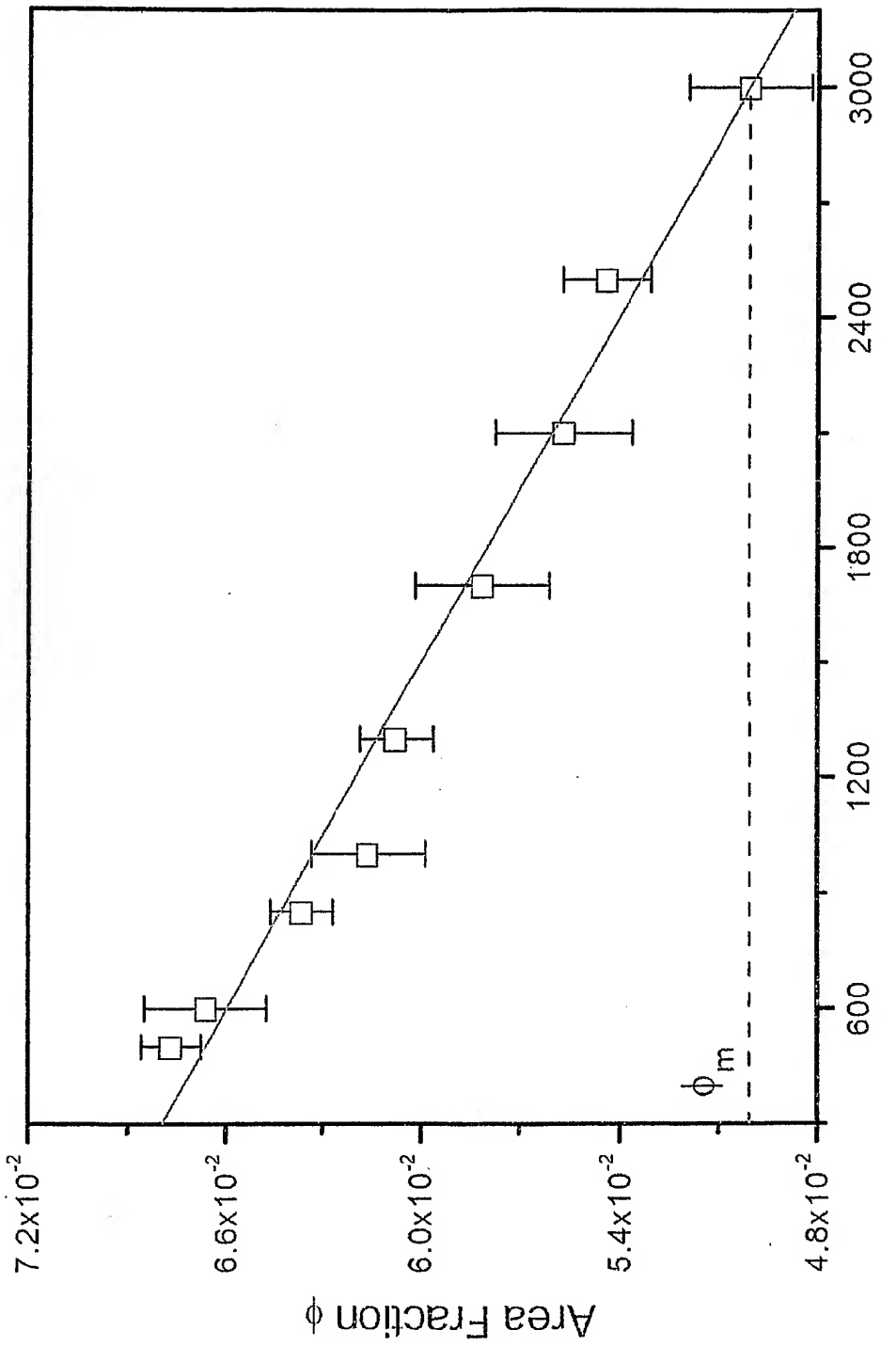
Area Fraction ϕ
7.2x10-2
6.6x10-2
6.0x10-2
5.4x10-2
4.8x10-2
ϕm
600
1200
1800
2400
3000
Frequency (Hz)

FIGURE 1d

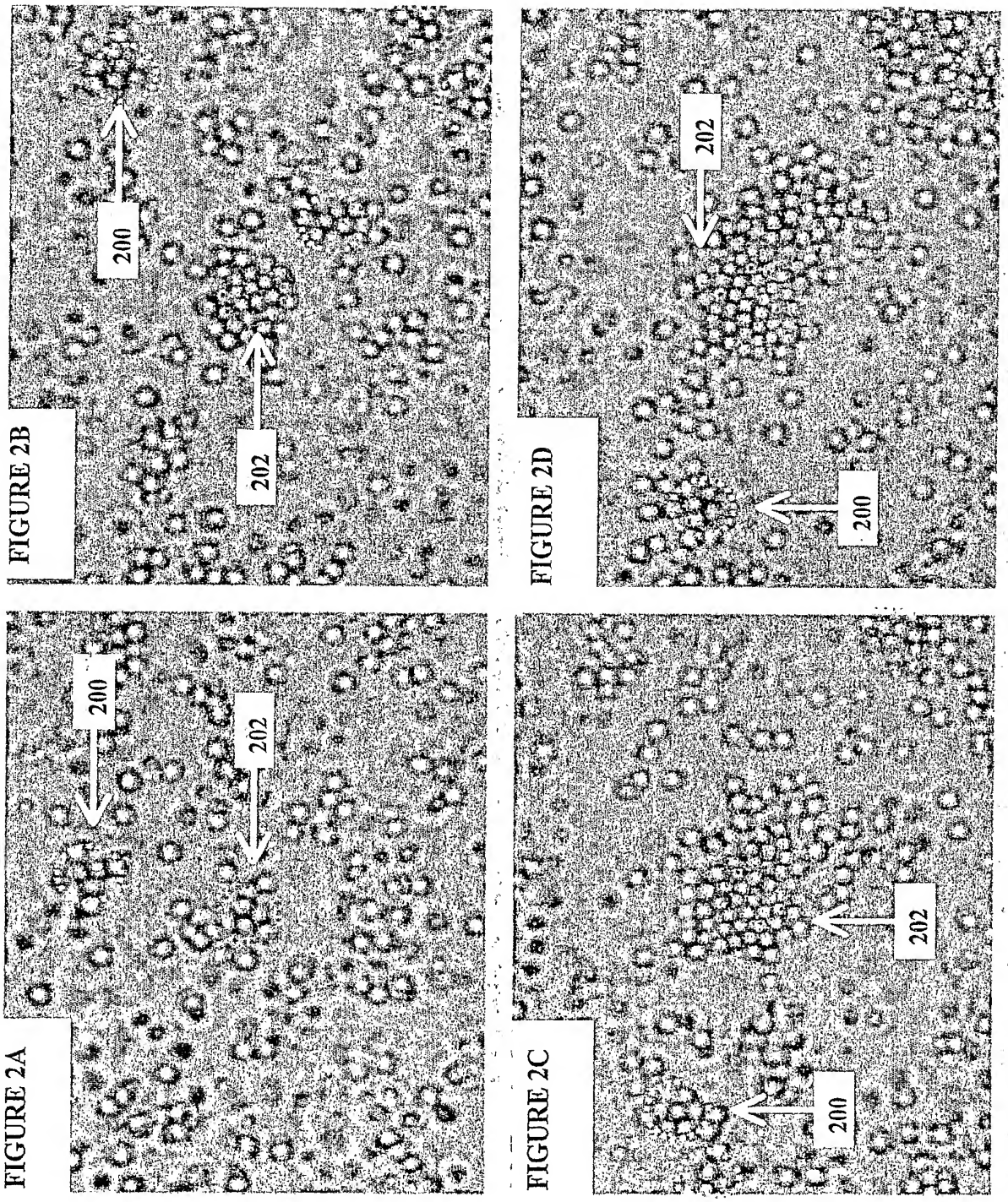
200
202
FIGURE 2A
200
202
FIGURE 2B
200
202
FIGURE 2C
200
202
FIGURE 2D

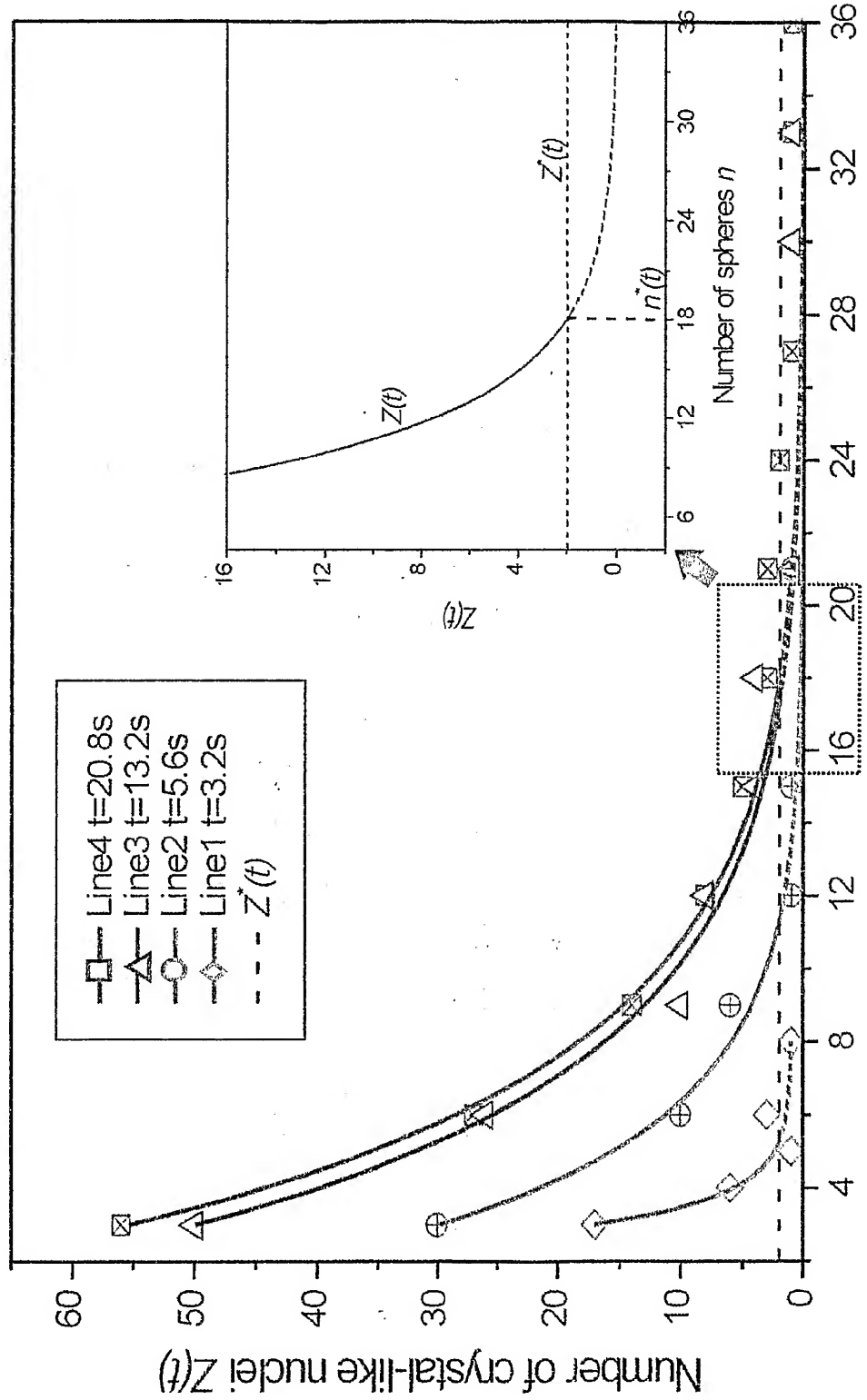
Number of crystal-like nuclei Z(t)
Number of spheres n
Line4 t=20.8s
Line3 t=13.2s
Line2 t=5.6s
Line1 t=3.2s
Z*(t)
Z(t)
Z*(t)
n*(t)
Number of spheres n

FIGURE 3a

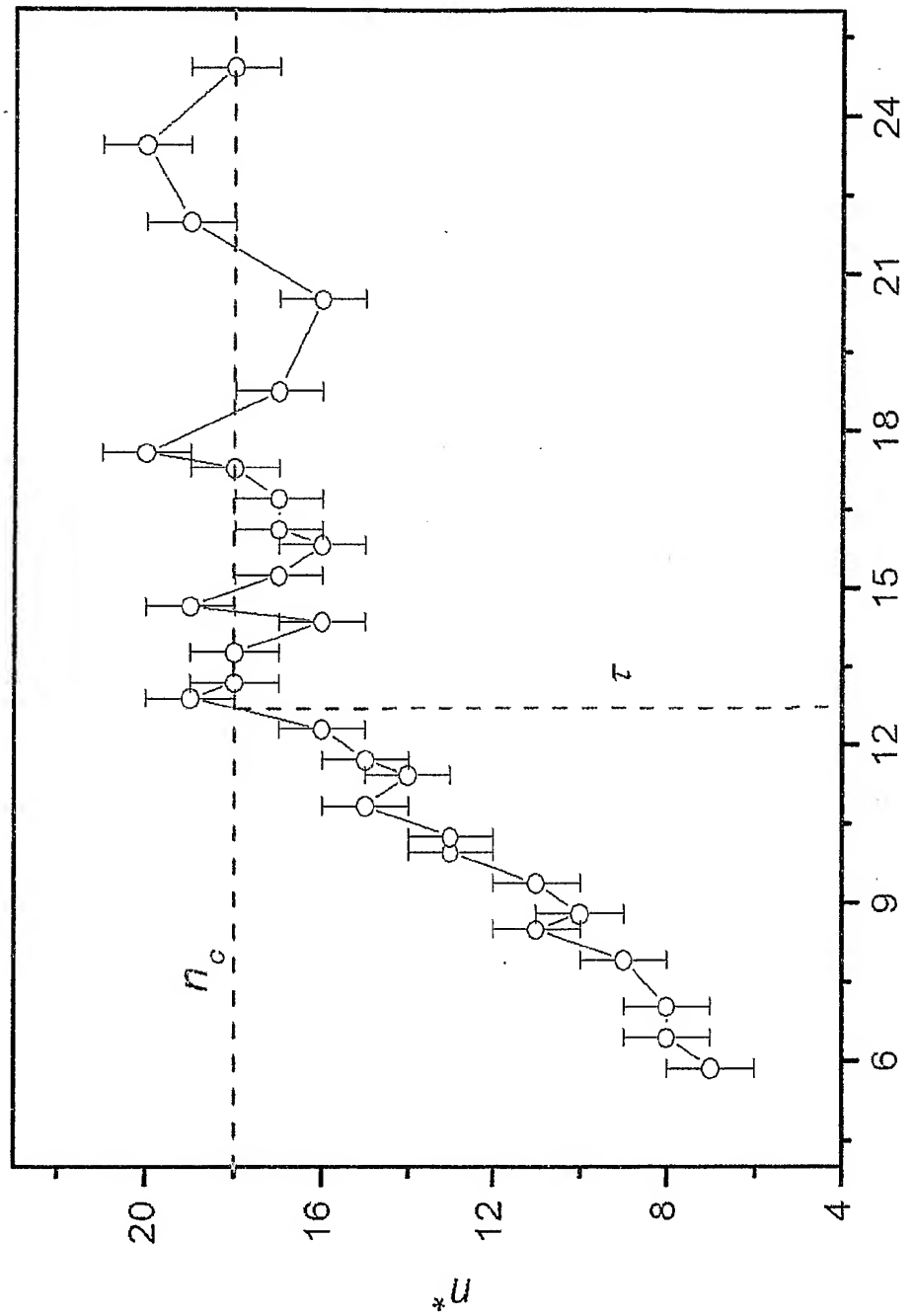

FIGURE 3b

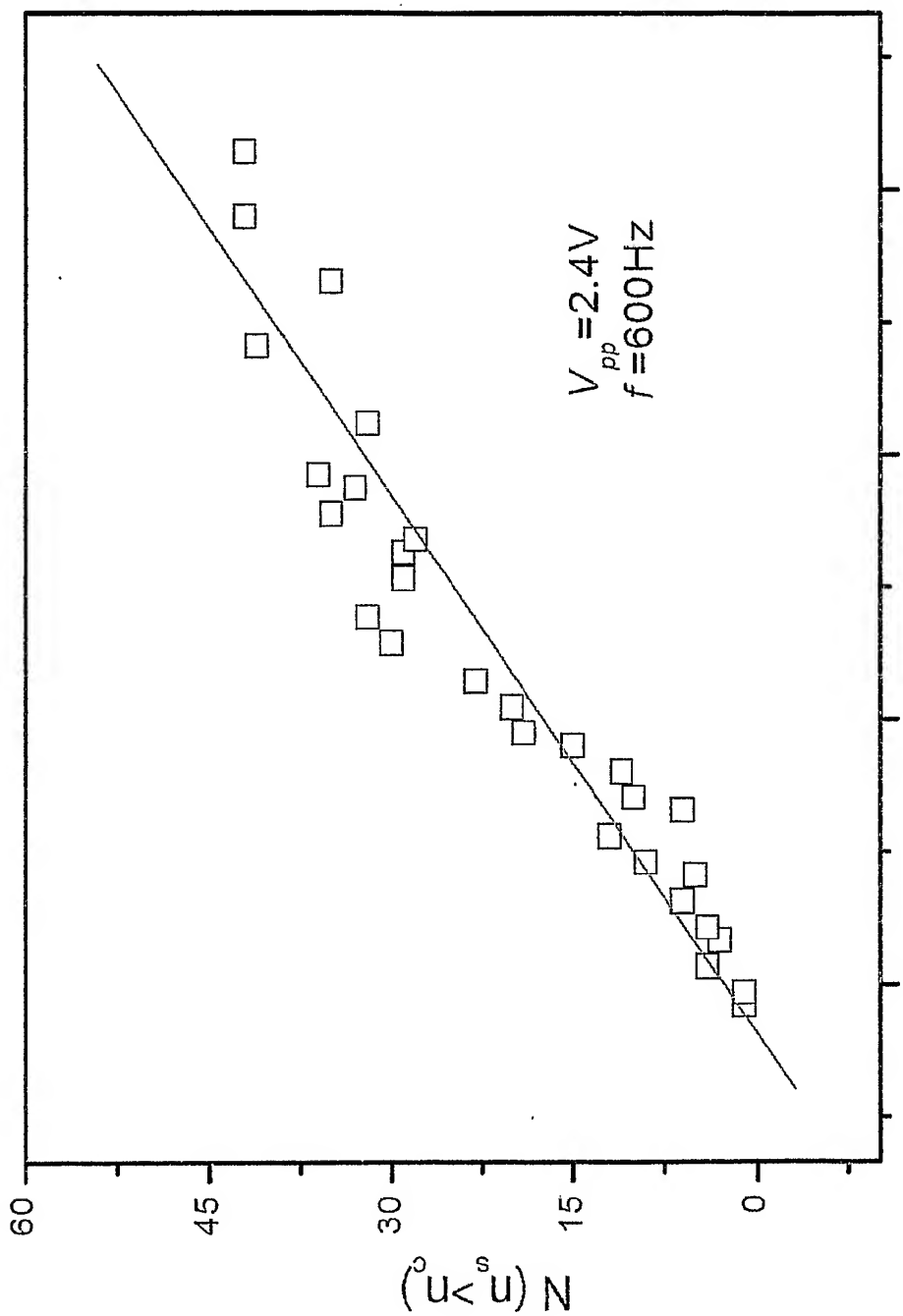

FIGURE 3c

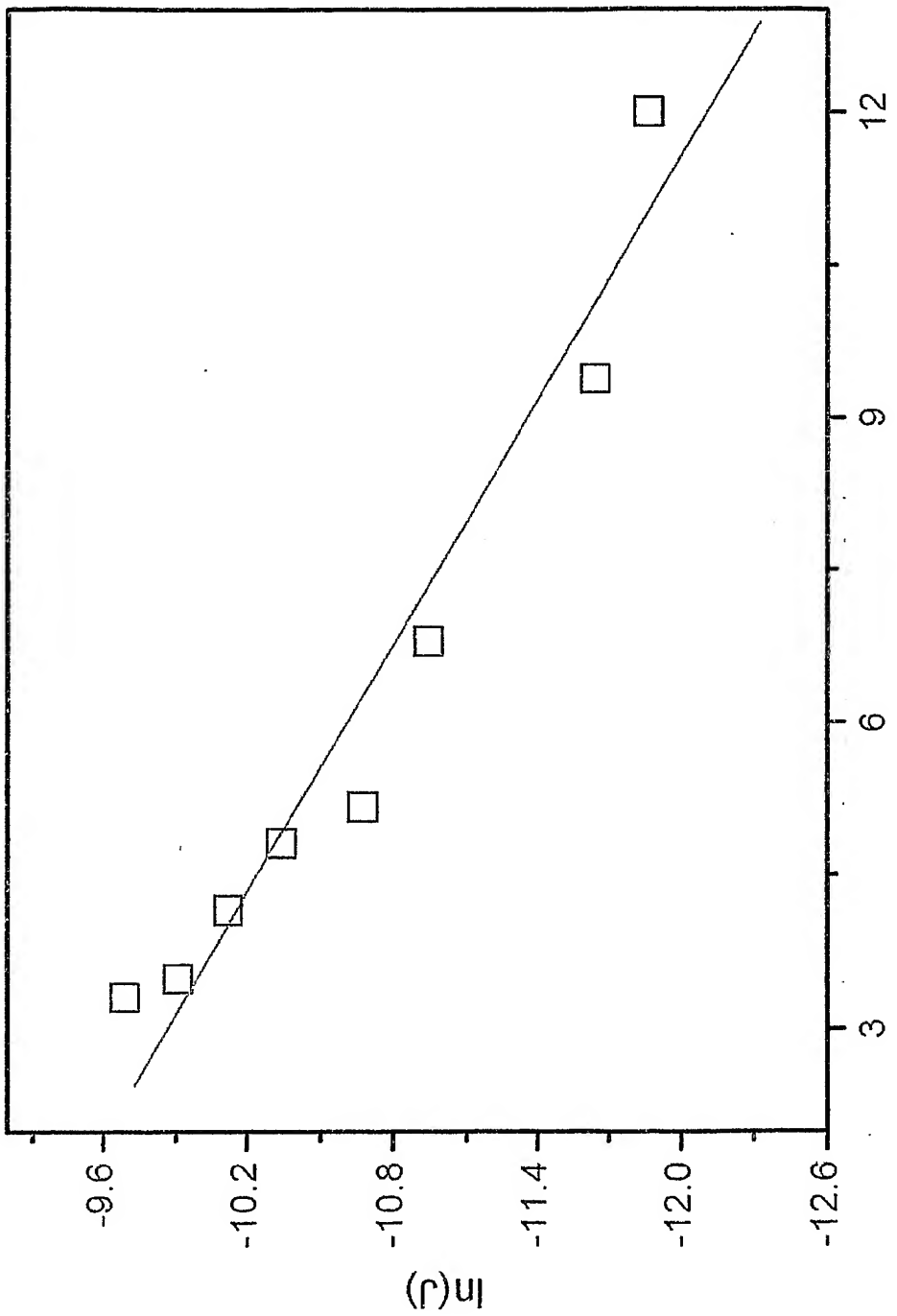

FIGURE 3d

FIGURE 4a

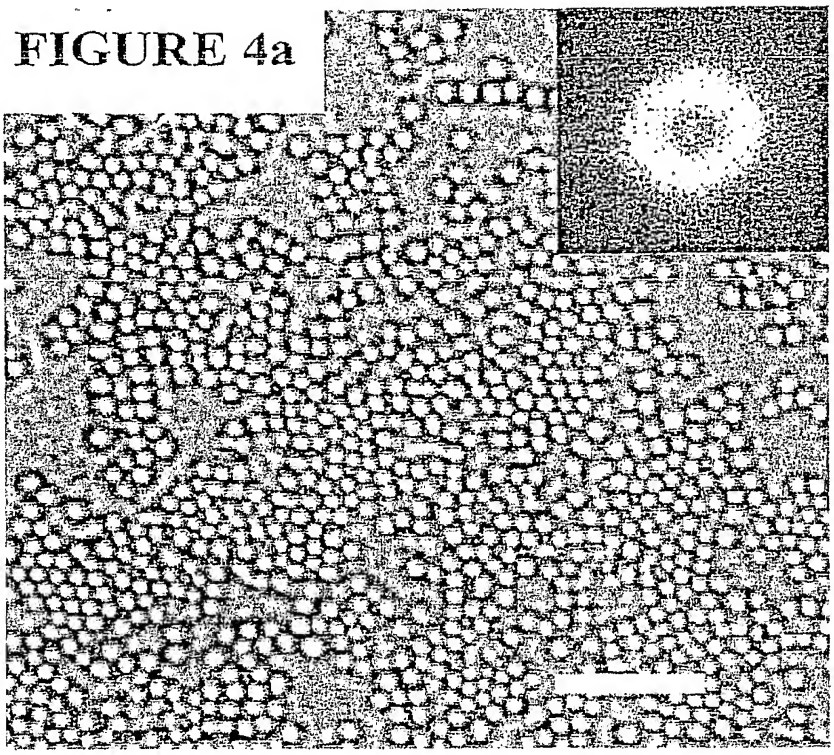

FIGURE 4b

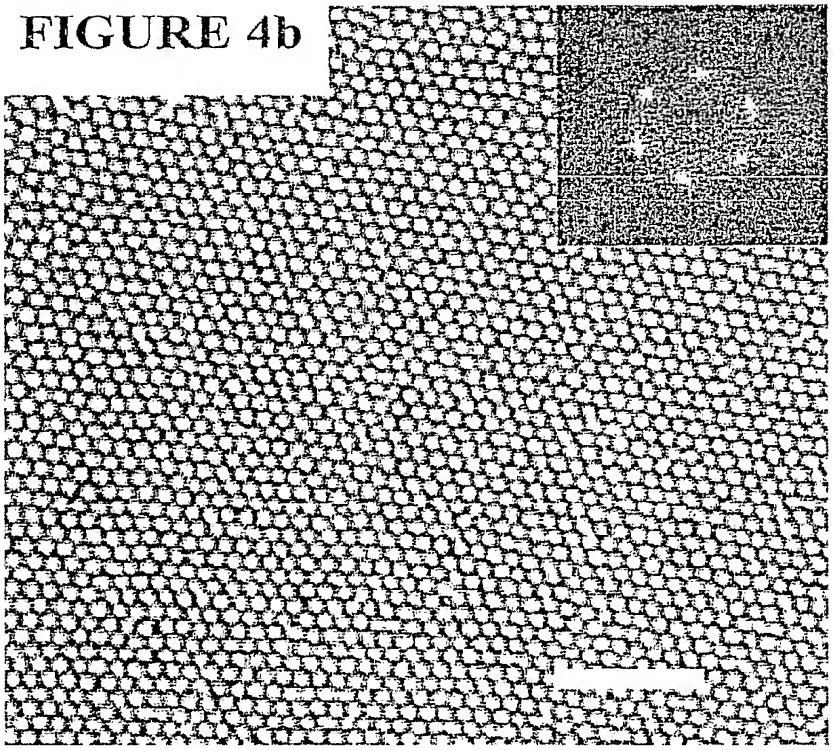

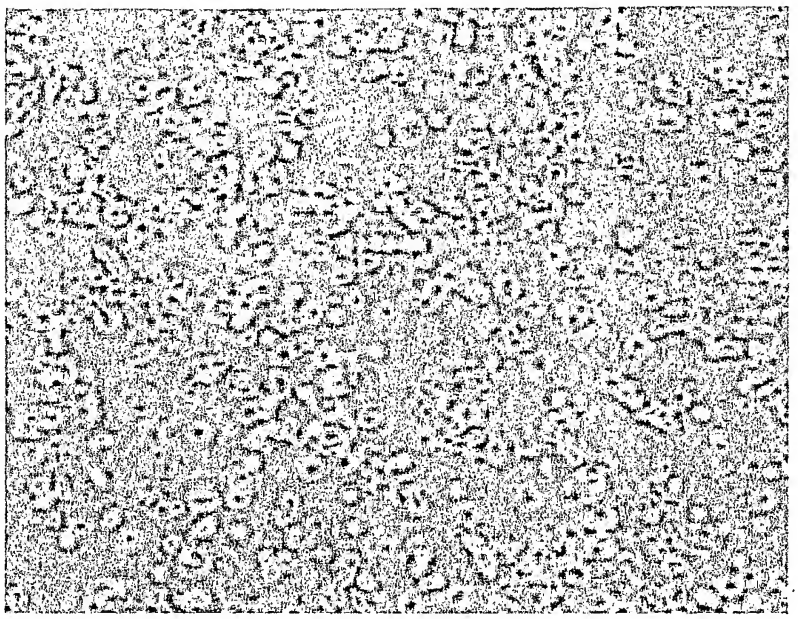

FIGURE 5

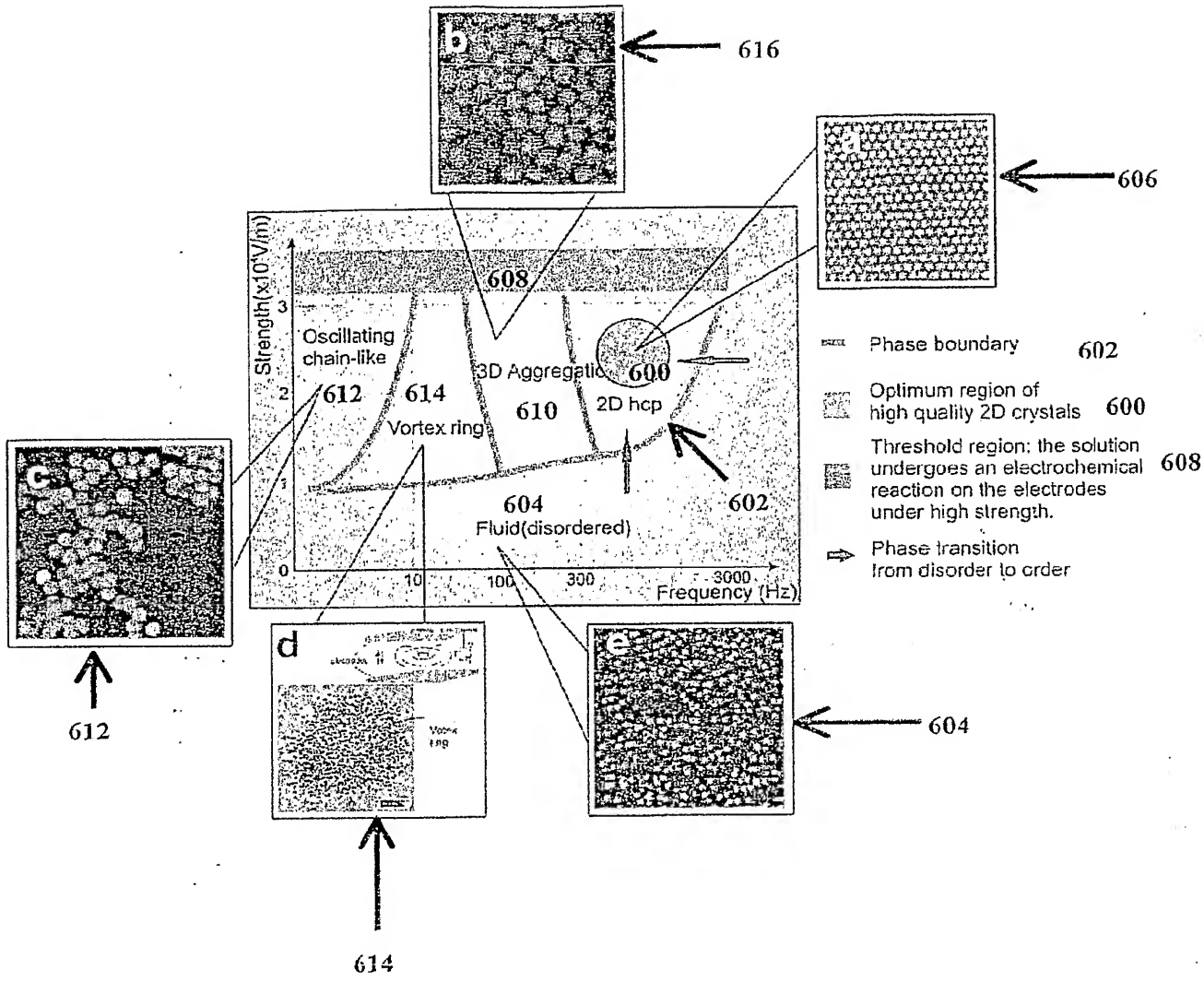
b
616
606
Strength(x10⁵V/m)
3
2
1
0
608
Oscillating chain-like
612
614
Vortex ring
3D Aggregati
600
610
2D hcp
604
Fluid(disordered)
602
10
100
300
3000
Frequency (Hz)
Phase boundary 602
Optimum region of high quality 2D crystals 600
Threshold region: the solution undergoes an electrochemical reaction on the electrodes under high strength. 608
Phase transition from disorder to order
c
612
d
e
604
614

FIGURE 6

FIGURE 7a

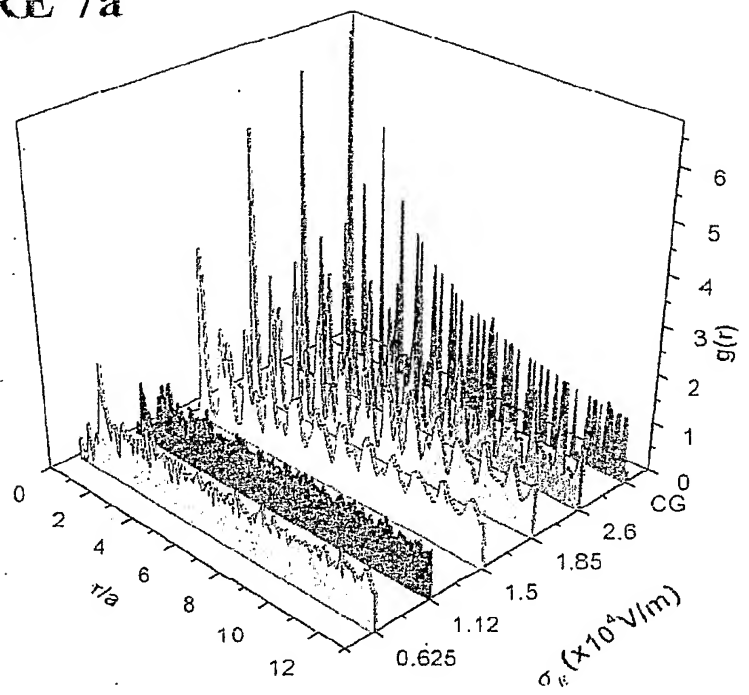

FIGURE 7b

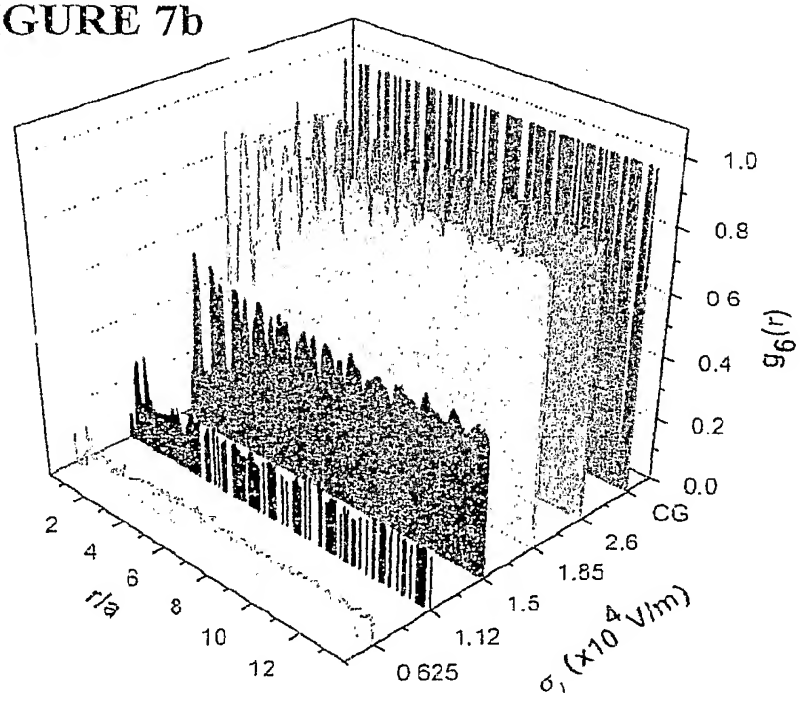

FIGURE 8a

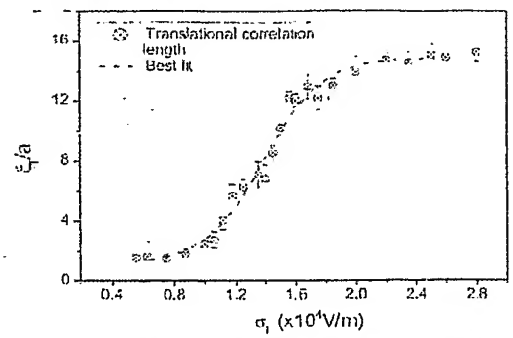

FIGURE 8b

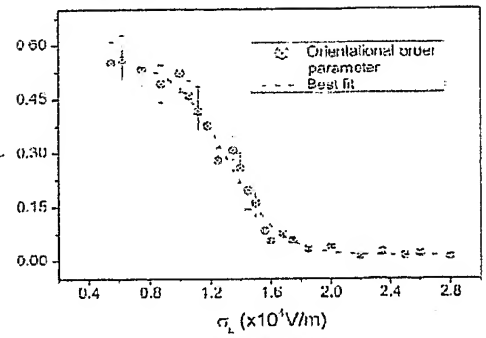

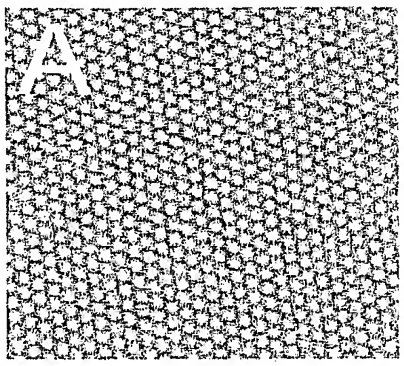

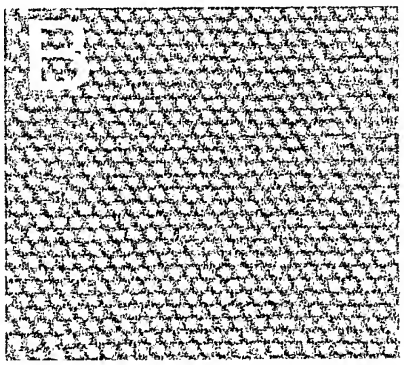

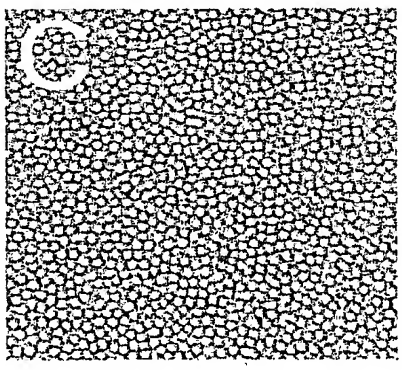

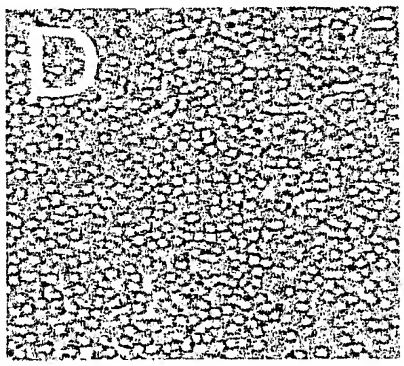

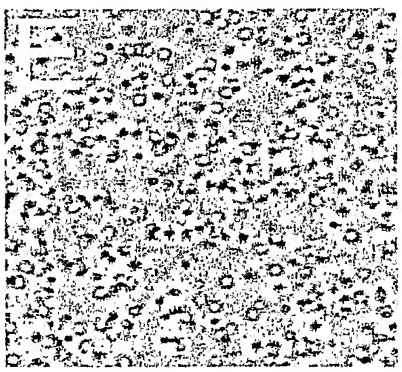

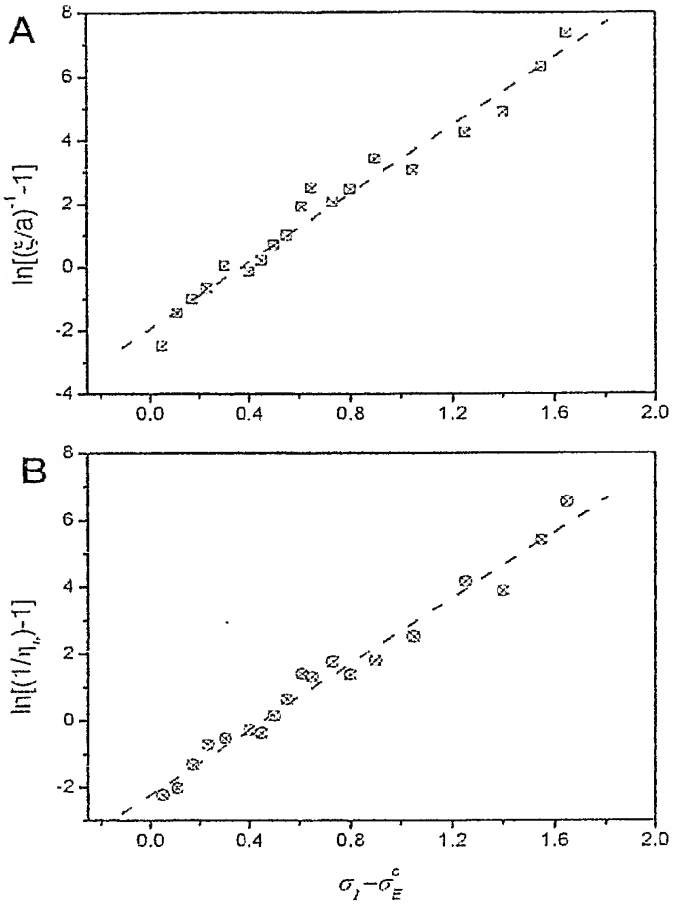

FIGURE 9

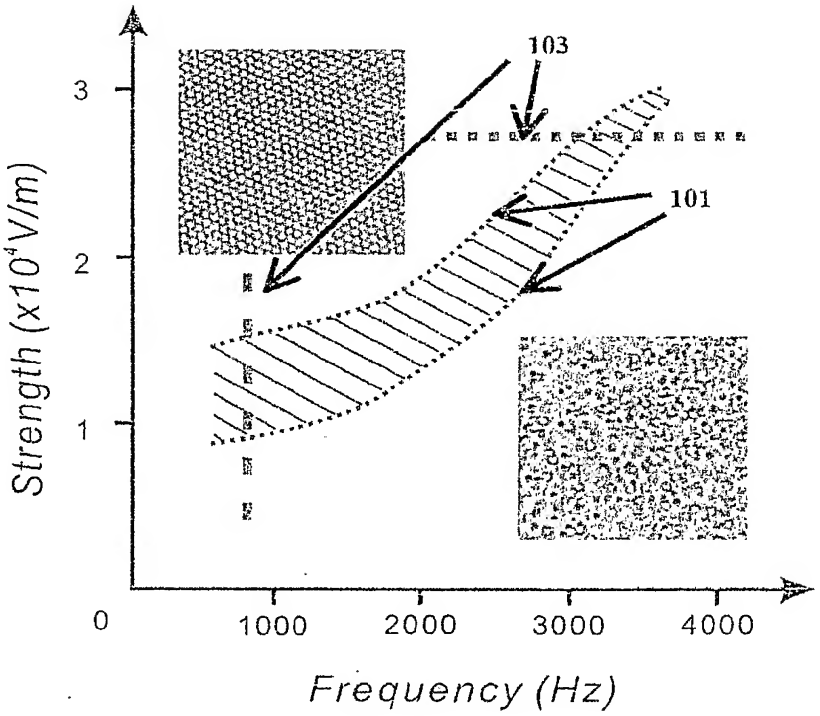
103
101
3
2
1
0
Strength (x10⁴V/m)
1000
2000
3000
4000
Frequency (Hz)

FIGURE 10

FIGURE 11a

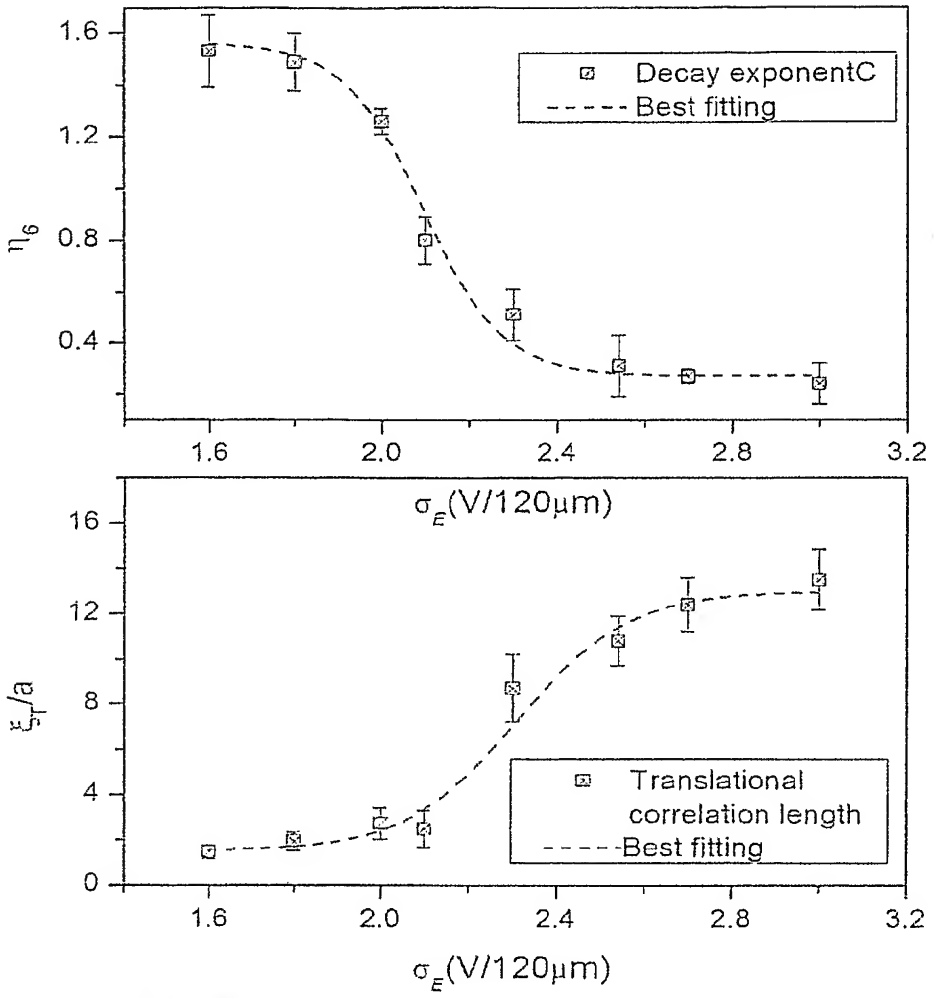

FIGURE 11b

FIGURE 11c

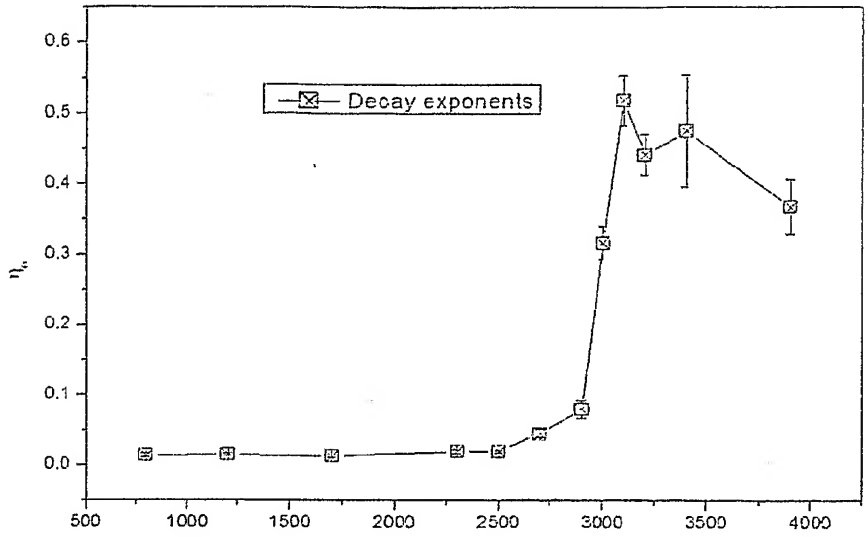

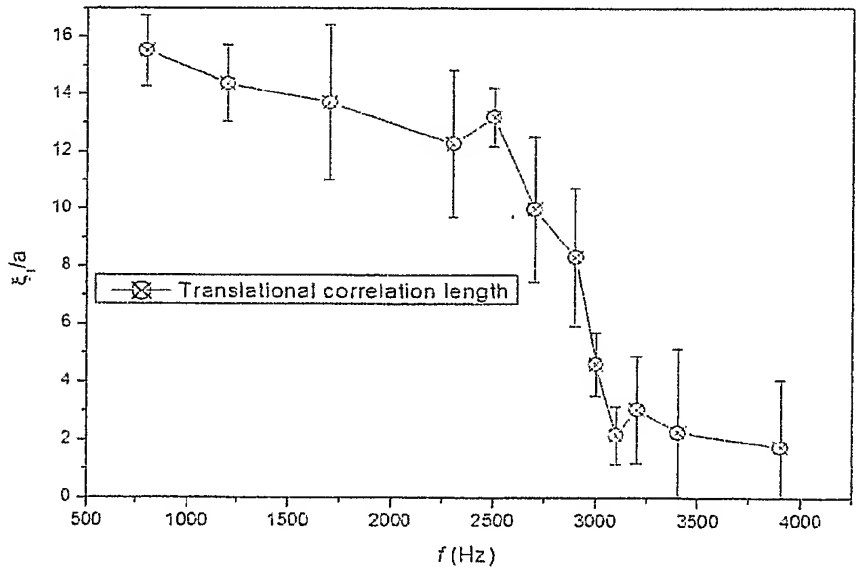

FIGURE 11d

FIGURE 12a

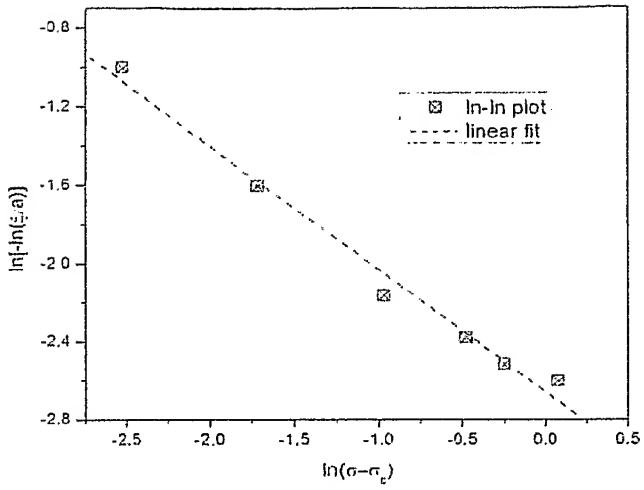

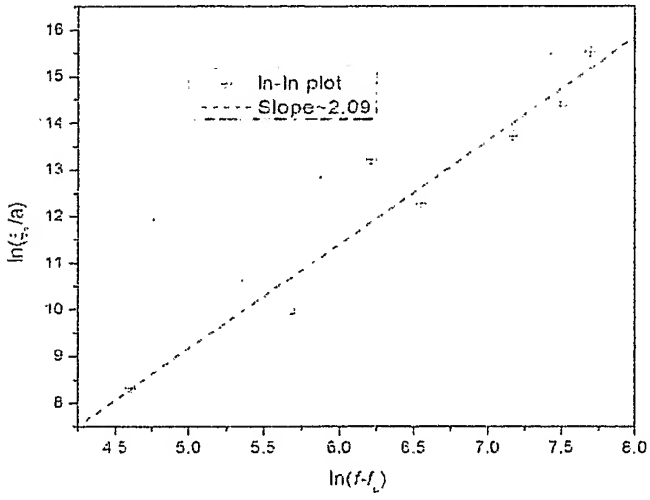

FIGURE 12b

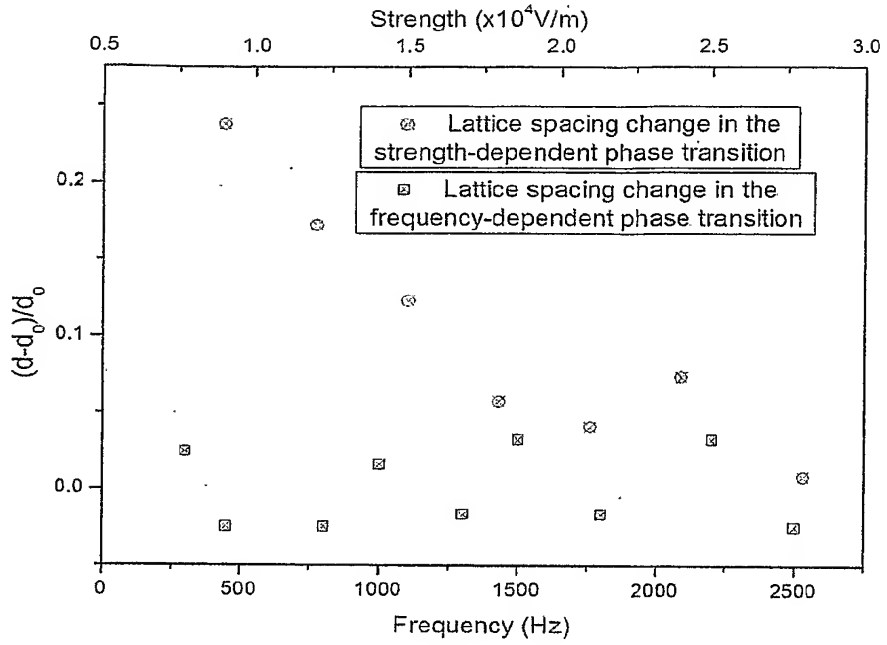
Strength (x10^{4}V/m)
0.5
1.0
1.5
2.0
2.5
3.0
Lattice spacing change in the strength-dependent phase transition
Lattice spacing change in the frequency-dependent phase transition
$(d-d_0)/d_0$
0.2
0.1
0.0
0
500
1000
1500
2000
2500
Frequency (Hz)

FIGURE 13

FIGURE 14a

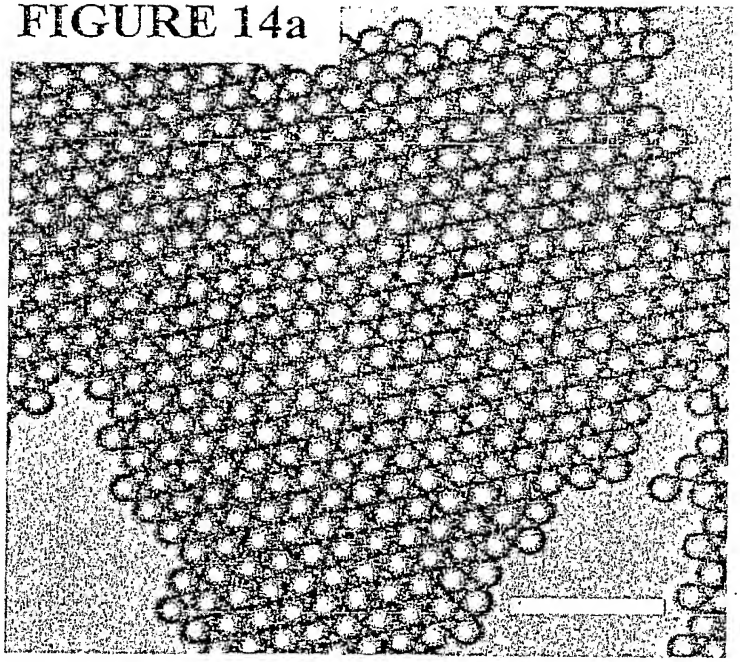

FIGURE 14b

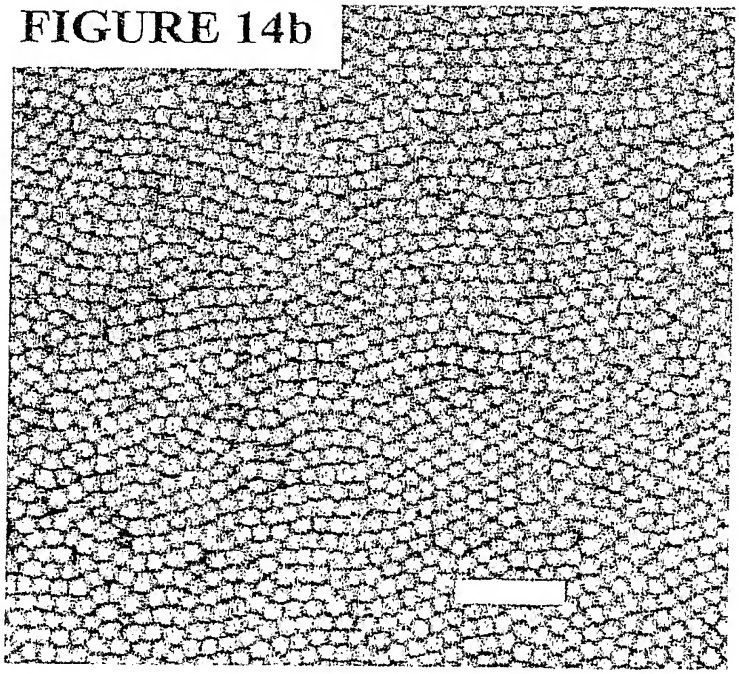

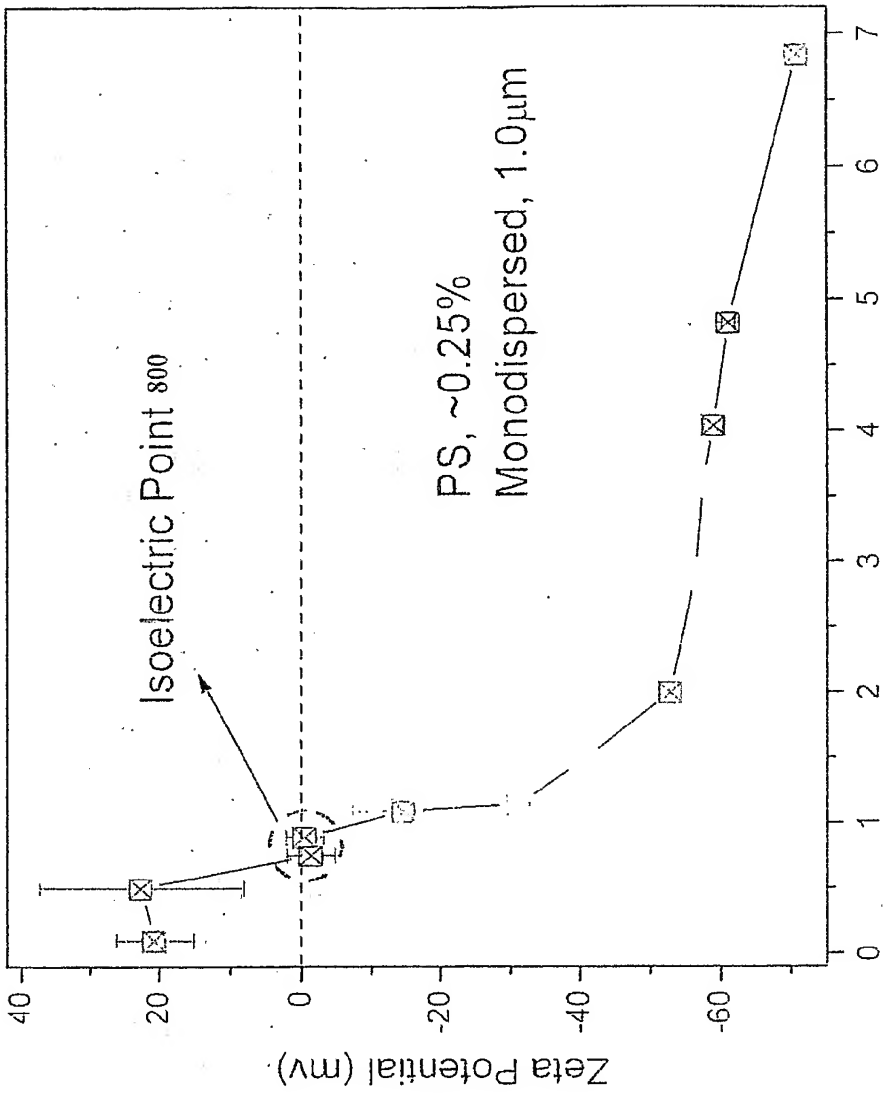
Isoelectric Point 800
PS, ~0.25%
Monodispersed, 1.0µm
Zeta Potential (mv)
40
20
0
-20
-40
-60
0
1
2
3
4
5
6
7
pH

FIGURE 15

INTERNATIONAL SEARCH REPORT

International application No.
PCT/SG2004/000369

A. CLASSIFICATION OF SUBJECT MATTER

Int. Cl. [7]: C30B 30/02; B01J 13/00

According to International Patent Classification (IPC) or to both national classification and IPC

B. FIELDS SEARCHED

Minimum documentation searched (classification system followed by classification symbols)
C30B 30/02: B01J 13/00

Documentation searched other than minimum documentation to the extent that such documents are included in the fields searched
NONE

Electronic data base consulted during the international search (name of data base and, where practicable, search terms used)
DWPI: C30B 30/02 or (B01J 13/00 and Keywords (CRYSTAL+ and ELECT+))

C. DOCUMENTS CONSIDERED TO BE RELEVANT

Category*	Citation of document, with indication, where appropriate, of the relevant passages	Relevant to claim No.
Y	WO 2003/080210 A (CENTRE NATIONAL DE LA RECHERCHE SCIENTIFIQUE) 2 October 2003 Whole document	18-31
Y	US 5084248 A (TAKENAKA, CHISATO) 28 January 1992 Whole document	18-31
Y	US 5477807 A (YAMADA, KAZUHIRO ET AL) 26 December 1995 Whole document	18-31
P, Y	WO 2004/081264 A (REIJONEN, MIKA T) 23 September 2004 Whole document	18-31

[X] Further documents are listed in the continuation of Box C [X] See patent family annex

* Special categories of cited documents:

"A" document defining the general state of the art which is not considered to be of particular relevance

"E" earlier application or patent but published on or after the international filing date

"L" document which may throw doubts on priority claim(s) or which is cited to establish the publication date of another citation or other special reason (as specified)

"O" document referring to an oral disclosure, use, exhibition or other means

"P" document published prior to the international filing date but later than the priority date claimed

"T" later document published after the international filing date or priority date and not in conflict with the application but cited to understand the principle or theory underlying the invention

"X" document of particular relevance; the claimed invention cannot be considered novel or cannot be considered to involve an inventive step when the document is taken alone

"Y" document of particular relevance; the claimed invention cannot be considered to involve an inventive step when the document is combined with one or more other such documents, such combination being obvious to a person skilled in the art

"&" document member of the same patent family

Date of the actual completion of the international search	Date of mailing of the international search report
18 January 2005	27 JAN 2005
Name and mailing address of the ISA/AU AUSTRALIAN PATENT OFFICE PO BOX 200, WODEN ACT 2606, AUSTRALIA E-mail address: pct@ipaustralia.gov.au Facsimile No. (02) 6285 3929	Authorized officer **GREGORY DIVEN** Telephone No : (02) 6283 2992

INTERNATIONAL SEARCH REPORT

International application No.
PCT/SG2004/000369

C (Continuation). DOCUMENTS CONSIDERED TO BE RELEVANT

Category*	Citation of document, with indication, where appropriate, of the relevant passages	Relevant to claim No.
Y	US 6221156 B (WATANABE, MASAHITO ET AL) 24 April 2001 Whole document	18-31
Y	US 6432198 B (WATANABE, MASAHITO ET AL) 13 August 2002 Whole document	18-31
Y	Derwent Abstract Accession No 2004-540832/52, Class J04, and KR 2004028360 A (KOREA ADVANCED INSTITUTE OF SCIENCE & TECHNOLOGY) 3 April 2004 Abstract	18-31
Y	Derwent Abstract Accession No 93-041400/05 Class v07, and JP 04367598 A (SUMITOMO ELECTRIC CO) 18 December 1992 Abstract	18-31
A	Derwent Abstract Accession No 1999-348537/30, Class L03 and DE 19857339 A (NEC CORP) 17 June 1999 Abstract	18-31
A	Derwent Abstract Accession No 95-285531/38, Class J04, L03 and JP 07172979 A (NEC CORP) 11 July 1995 Abstract	18-31
A	Derwent Abstract Accession No 2001-391492/42, Class A89, G06, L03 and EP 1081513 A (LUCENT TECHNOLOGIES INC) 7 March 2001 Abstract	18-31
A	Derwent Abstract Accession No 2002-741957/81, Class J04 and CN136418 A (UNIV HUANAN SCI & ENG) 14 August 2002 Abstract	18-31
A	Derwent Abstract Accession No 92-189172/23, Class X12 and JP04124084 A (HAMAMATSU PHOTONICS KK) 24 April 1992 Abstract	18-31

INTERNATIONAL SEARCH REPORT

International application No.
PCT/SG2004/000369

Box No. II Observations where certain claims were found unsearchable (Continuation of item 2 of first sheet)

This international search report has not been established in respect of certain claims under Article 17(2)(a) for the following reasons:

1. [X] Claims Nos.: **1-17**

because they relate to subject matter not required to be searched by this Authority, namely:

The claims relate to the optimization of conditions to grow crystals and as such are not suitable subject matter for the grant of a patent. They amount to nothing more than trial and error.

2. [ ] Claims Nos.:

because they relate to parts of the international application that do not comply with the prescribed requirements to such an extent that no meaningful international search can be carried out, specifically:

3. [ ] Claims Nos.:

because they are dependent claims and are not drafted in accordance with the second and third sentences of Rule 6.4(a)

Box No. III Observations where unity of invention is lacking (Continuation of item 3 of first sheet)

This International Searching Authority found multiple inventions in this international application, as follows:

1. [ ] As all required additional search fees were timely paid by the applicant, this international search report covers all searchable claims.
2. [ ] As all searchable claims could be searched without effort justifying an additional fee, this Authority did not invite payment of any additional fee.
3. [ ] As only some of the required additional search fees were timely paid by the applicant, this international search report covers only those claims for which fees were paid, specifically claims Nos.:
4. [ ] No required additional search fees were timely paid by the applicant. Consequently, this international search report is restricted to the invention first mentioned in the claims; it is covered by claims Nos.:

Remark on Protest

[ ] The additional search fees were accompanied by the applicant's protest.

[ ] No protest accompanied the payment of additional search fees.

INTERNATIONAL SEARCH REPORT

Information on patent family members

International application No.
PCT/SG2004/000369

This Annex lists the known "A" publication level patent family members relating to the patent documents cited in the above-mentioned international search report. The Australian Patent Office is in no way liable for these particulars which are merely given for the purpose of information.

Patent Document Cited in Search Report		Patent Family Member					
WO	2003080210	FR	2837400				
US	5084248	JP	02006383				
US	5477807	DE	69418119	EP	0643158	JP	07126100
		KR	137085				
WO	2004081264	FI	20030394	FI	20030576	FI	20031117
		FI	20040327				
US	6221156	DE	19911755	JP	11263691	US	6432198
US	6432198	DE	19911755	JP	11263691	US	6221156
KR	2004028360		NONE				
JP	04367598		NONE				
DE	19857339	JP	11171686	US	6077346		
JP	07172979		NONE				
EP	1081513	CA	2317371	JP	2001162157	US	6436187
CN	1363418		NONE				
JP	04124084		NONE				

Due to data integration issues this family listing may not include 10 digit Australian applications filed since May 2001.

END OF ANNEX